Asymptotic SER Analysis and Optimal Power Sharing for Dual-Phase and Multi-Phase Multiple-Relay Cooperative Systems

Neeraj Varshney, *Student Member, IEEE*, Aditya K. Jagannatham, *Member, IEEE*, and Lajos Hanzo, *Fellow, IEEE*

***Abstract*—The asymptotic high-SNR symbol error rate (SER) performance of selective decode-and-forward (DF) cooperative multiple relay aided wireless systems is derived for M-PSK and M-QAM modulations. The proposed analysis considers both dual-phase and multi-phase relaying protocols. Furthermore, analytical results are also presented for optimal power allocation both at the source and at each of the relays, since it significantly influences the performance of cooperative communication. A novel aspect of the proposed framework is that the SER and optimal power allocation results derived are applicable to diverse fading channels such as $\eta-\mu$, $\kappa-\mu$, shadowed-Rician scenarios and each for non-identical fading for the source-destination (SD), source-relay (SR), and relay-destination (RD) links. The applicability of the proposed framework is also demonstrated for diverse PHY layer schemes, such as multiple-input multiple-output (MIMO)-orthogonal space time block codes (OSTBCs), cooperative beamforming, joint transmit/receive antenna selection, free space optical (FSO) scenarios etc. This high-SNR analysis provides valuable insights into the impact of the diversity orders of the SR and RD links on the end-to-end SER as well as on the optimal power allocation factors both in the dual-phase and multi-phase protocols of various fading channels and schemes. Our simulation results verify the analytical results derived.**

***Index Terms*—Arbitrary fading model, cooperative beamforming, FSO, MIMO, OSTBC, transmit-receive antenna selection, unified framework, zero-forcing.**

I. Introduction

COOPERATIVE communication [2]–[5] relying on multiple spatially separated relay nodes, has gained significant popularity due to its ability to enhance the coverage area as a benefit of its high diversity gain. On a similar note, cooperative communication is also capable of significantly enhancing the reliability, lifetime and throughput of communication networks. Amongst the various protocols proposed for cooperative communications, selective decode-and-forward (DF) [2], [6], that relays the symbols only when the signal to noise ratio (SNR) is above a threshold, has been shown to be particularly resilient to error propagation. In this context, the authors of [6]–[18] have analyzed the performance of multi-relay cooperative scenarios in terms of their symbol error rate (SER), outage probability etc. However, majority of contributions in the literature consider specific fading scenarios in conjunction with a fixed physical (PHY) layer transmission scheme. Another idealized simplifying assumption that the source-destination (SD), source-relay (SR), and relay-destination (RD) links fade identically, which limits their applicability and prevents the extension of results to other fading scenarios.

In order to circumvent the above limitations in the literature, we present a simplified analytical framework based on a polynomial high-SNR approximation of the fading channel's probability density function (PDF) described in [19] to characterize the high-SNR performance of both dual-phase ($\mathcal{P}_0$) and multi-phase ($\mathcal{P}_m$) multi-relay selective DF systems for several channels such as Nakagami, Weibull, Shadowed-Rician, $\kappa-\mu$ fading etc. The advantage of the proposed analysis is that our results characterize both the end-to-end SER, the diversity order as well as the optimal power allocation for several popular techniques such as multiple-input multiple-output (MIMO)-orthogonal space time block codes (OSTBCs), cooperative beamforming, transmit/ receive antenna selection etc. and hence it is not restricted to a specific scheme. Our generalized framework assists in consolidating and comparing the performance of cooperative communications for a wide range of fading channels, and PHY layer techniques. A brief review of existing treatises in this context is presented next.

A. Related Work

Zhao et al. [7] presented the outage analysis of selective DF systems communicating over Rayleigh faded links. However, the analysis therein is restricted to single antenna nodes. Closed-form expressions have been derived by Hu and Beaulieu [8] for both the outage and error probabilities of selective DF relaying over dissimilar Rayleigh fading channels using multiple relays without considering optimal power allocation. An asymptotic approximation for the outage probability has been derived by Li and Kishore [9] to quantify the diversity order and coding gain of a multi-relay amplify-and-forward (AF) cooperative system communicating over Nakagami-m fading channels. In [10], [11], the high-SNR end-to-end performance of a selective DF based multi-relay cooperative system has been analyzed by Soleimani-Nasab et al. over independent Nakagami-m and Rician fading links, respectively. The system

The proposed framework considering the single relay based path selection scheme has appeared in a conference paper [1].

Neeraj Varshney and Aditya K. Jagannatham are with the Department of Electrical Engineering, Indian Institute of Technology Kanpur, Kanpur UP 208016, India (e-mail: neerajv@iitk.ac.in; adityaj@iitk.ac.in).

Lajos Hanzo is with the School of Electronics and Computer Science, University of Southampton, Southampton, SO17 1BJ, UK (email: lh@ecs.soton.ac.uk).

The financial support of the EPSRC projects EP/Noo4558/1, EP/PO34284/1 as well as of the European Research Council's Advanced Fellow Grant QuantCom is gratefully acknowledged.

model of [9] considers only a single antenna at each of the relays, while [10], [11] assume two antennas at each relay, with single antenna source and destination nodes. Hence, the results therein cannot be readily generalized to nodes with an arbitrary number of antennas. A two-phase multi-relay single-input single-output (SISO) cooperative beamforming system has been analyzed in terms of its outage probability and bit error rate (BER) by Hong et al. [12]. Hesam et al. [13] recently conceived a cooperative beamforming technique and analyzed its BER. However, these works are restricted to Rayleigh fading links and cannot be readily extended to other fading scenarios. Moreover, the optimal power allocation has not been presented. The authors of [6], [14] presented the analysis of a class of multi-phase multi-relay DF cooperative protocols $C(m); 1 \leq m \leq M-1$, with M denoting the number of relays, in which each relay combines the signals received both from the source and from a subset of previous relays. However, the SER and power allocation analyses therein have only been presented for single antenna nodes over Rayleigh faded links. Thus, there is a void in existing research in terms of a general framework for the analysis of multi-relay cooperative systems, which is applicable to a broad variety of fading channels and PHY layer schemes.

B. Contributions and Organization of the Paper

We propose a simplified framework for the SER and optimal power allocation analysis of selective DF based cooperative communication systems using multiple relays, that is applicable for various fading scenarios and transmission schemes relying on M-QAM/ M-PSK modulation. The polynomial approximation of the fading channel's PDF of Wang and Giannakis [19] is described in Section II-A, which provides accurate parameterizations for diverse fading channel PDFs. This is used for quantifying the key performance metrics of cooperative wireless system. Closed-form expressions are derived both for the asymptotic end-to-end SER and for the diversity order of our dual-phase ($\mathcal{P}_0$) and multi-phase ($\mathcal{P}_m$) protocols in Sections II-B and III-B, respectively. We also derive the optimal source and relay power allocation for end-to-end error rate minimization in Sections II-B1 and III-B1. The impact of the diversity orders of the SR and RD links on the end-to-end SER as well as on the optimal power fractions is explicitly demonstrated for both the dual-phase and multi-phase protocols. A novel aspect of the work is that the analytical results derived are not restricted to any particular PHY layer scheme and their applicability is explicitly demonstrated for both single as well as multiple antenna nodes relying on MIMO-OSTBCs, MIMO-zero forcing (ZF), cooperative beamforming, free-space optical (FSO) links etc in Section IV. The simulation results of Section V demonstrate the performance of the cooperative systems under consideration, while simultaneously verifying the analytical results.

The following notation is used in the rest of the presentation. The quantity $\mathbf{A}^H$ denotes the Hermitian transpose of the matrix $\mathbf{A}$, $|a|$ represents the magnitude of the complex number a, $\|\mathbf{A}\|_F$ denotes the matrix Frobenius norm given by $\|\mathbf{A}\|_F = \sqrt{\text{Tr}(\mathbf{A}\mathbf{A}^H)}$, where $\text{Tr}(\cdot)$ is the trace of a square matrix. The symbol $\doteq$ is used to represent the high-SNR approximation. Finally, $\mathbb{E}\{\cdot\}$ denotes the expectation operator and $\mathbb{C}^{N\times M}$ denotes the space of $(N \times M)$ matrices over the complex field $\mathbb{C}$. In addition, the complete list of acronyms used in this work is given in Table I.

TABLE I
List of Acronyms

Acronym	Description
SER	Symbol Error Rate
SNR	Signal to Noise Ratio
DF	Decode-and-Forward
M-PSK	M-ary Phase-Shift Keying
M-QAM	M-ary Quadrature Amplitude Modulation
SD	Source-Destination
SR	Source-Relay
RD	Relay-Destination
PHY	Physical
MIMO	Multiple-Input Multiple-Output
OSTBC	Orthogonal Space Time Block Code
FSO	Free Space Optical
PDF	Probability Density Function
AF	Amplify-and-Forward
SISO	Single-Input Single-Output
BER	Bit Error Rate
ZF	Zero Forcing
TAs	Transmitter Antennas
CSI	Channel State Information
QPSK	Quadrature Phase Shift Keying
GP	Geometric Program
KKT	Karush-Kuhn-Tucker
AWGN	Additive White Gaussian Noise
SIM	Subcarrier Intensity Modulation
LMS	Land Mobile Satellite

II. $\mathcal{P}_0$ BASED SELECTIVE DF RELAYING

This section begins by describing our cooperative communication model for the dual-phase multiple-relay protocol $\mathcal{P}_0$. The analysis of the multi-phase multi-relay protocol $\mathcal{P}_m$ using inter-relay communication is subsequently described in Section III. It is also worth noting that the results for the dual-phase protocol $\mathcal{P}_0$ cannot be derived as a special case of the multi-phase protocol $\mathcal{P}_m$, since the dual-phase protocol involves a single phase for the transmission of multiple relays. By contrast, the multi-phase protocol has several phases, with a single relay transmitting in each stage based on combining the information of one or more relays from the previous stages.

A. System Model

Consider now a selective DF cooperative wireless scenario with a source (S)-destination (D) node pair in addition to R relay nodes $R_1, R_2, \cdots, R_R$, as shown in Fig. 1. The cooperative relaying protocol $\mathcal{P}_0$ is described as follows. In the initial phase, the source broadcasts an information symbol to the R relays and destination nodes with power P_0. In the subsequent relaying phase, the group of R relays employ selective DF based retransmission, wherein the relays forward the symbol to the destination node with power $P_r, 1 \leq r \leq R$ only if the decoding SNR exceeds the reliable decoding threshold, similar to [6], [14], [21]. The source-destination, source-r^{th} relay, and r^{th} relay-destination wireless links are assumed to be fading

Fading Channel	**PDF** $f(\beta)$	t	a
Rayleigh	$\frac{1}{\delta^2}\exp\left(-\frac{\beta}{\delta^2}\right)$	0	$\frac{1}{\delta^2}$
Rician, $K \geq 0$	$\frac{(1+K)}{\delta^2}\exp(-K)\exp\left(-\frac{(1+K)\beta}{\delta^2}\right) I_0\left(2\sqrt{\frac{K(1+K)\beta}{\delta^2}}\right)$	0	$\frac{(1+K)}{\delta^2}\exp\left(-K\right)$
Generalized Nakagami, $s>0, m \geq \frac{1}{2}$	$\frac{s\beta^{ms-1}}{p^m\Gamma(m)}\exp\left(-\frac{s\beta}{p}\right)$, where $p=\left(\frac{\delta^2\Gamma(m)}{\Gamma(m+s^{-1})}\right)^s$	$ms-1$	$\frac{s}{p^m\Gamma(m)}$
Nakagami-q (Hoyt), $0 \leq q \leq 1$	$\frac{(1+q^2)}{2q\delta^2}\exp\left(-\frac{(1+q^2)^2\beta}{4q^2\delta^2}\right) I_0\left(\frac{(1-q^4)\beta}{4q^2\delta^2}\right)$	0	$\frac{1+q^2}{2q\delta^2}$
Nakagami-n (Rice), $n \geq 0$	$\frac{(1+n^2)}{\delta^2}\exp(-n^2)\exp\left(-\frac{(1+n^2)\beta}{\delta^2}\right) I_0\left(2n\sqrt{\frac{(1+n^2)\beta}{\delta^2}}\right)$	0	$\frac{(1+n^2)}{\delta^2}\exp\left(-n^2\right)$
Weibull, c	$\frac{c}{2}\left(\frac{\Gamma\left(1+\frac{2}{c}\right)}{\delta^2}\right)^{c/2}\beta^{\frac{c}{2}-1}\exp\left(-\left(\frac{\beta}{\delta^2}\Gamma\left(1+\frac{2}{c}\right)\right)^{c/2}\right)$	$\frac{c}{2}-1$	$\frac{c}{2}\left(\frac{\Gamma\left(1+\frac{2}{c}\right)}{\delta^2}\right)^{\frac{c}{2}}$
Log-Normal, σ	$\frac{4.34}{\sqrt{2\pi}\sigma\beta}\exp\left[-\frac{(10\log_{10}\beta-\mu)^2}{2\sigma^2}\right]$	$\frac{\mu}{\sigma^2}-1$	$\frac{4.34}{\sqrt{2\pi}\sigma}\exp\left(-\frac{\mu^2}{2\sigma^2}\right)$
Shadowed-Rician, b, m, Ω	$\frac{0.5}{b}\left(\frac{2bm}{2bm+\Omega}\right)^m\exp\left(-\frac{\beta}{2b}\right){}_1F_1\left(m,1;\frac{0.5\Omega}{(2b^2m+b\Omega)}\beta\right)$	0	$\frac{0.5}{b}\left(\frac{2bm}{2bm+\Omega}\right)^m$
κ-μ distribution, κ, μ [20]	$\frac{\mu(1+\kappa)^{\frac{\mu+1}{2}}\beta^{\frac{\mu-1}{2}}}{\kappa^{\frac{\mu-1}{2}}\exp(\mu\kappa)(\delta^2)^{\frac{\mu+1}{2}}}\exp\left(-\frac{\mu(1+\kappa)\beta}{\delta^2}\right) I_{\mu-1}\left(2\mu\sqrt{\frac{\kappa(1+\kappa)\beta}{\delta^2}}\right)$	$\mu-1$	$\frac{(\mu(1+\kappa))^\mu}{\exp(\mu\kappa)(\delta^2)^\mu\Gamma(\mu)}$
η-μ distribution, η, μ [20]	$\frac{2\sqrt{\pi}\mu^{\mu+\frac{1}{2}}h^\mu\beta^{\mu-\frac{1}{2}}}{\Gamma(\mu)H^{\mu-\frac{1}{2}}(\delta^2)^{\mu+\frac{1}{2}}}\exp\left(-\frac{2\mu h\beta}{\delta^2}\right) I_{\mu-\frac{1}{2}}\left(\frac{2\mu H\beta}{\delta^2}\right)$, For format 1: $0<\eta<\infty$, $h=\frac{2+\eta^{-1}+\eta}{4}, H=\frac{\eta^{-1}-\eta}{4}$ For format 2: $-1<\eta<1$, $h=\frac{1}{1-\eta^2}, H=\frac{\eta}{1-\eta^2}$	$2\mu-1$	$\frac{2\sqrt{\pi}\mu^{2\mu}h^\mu}{\Gamma(\mu)\Gamma(\mu+0.5)(\delta^2)^{2\mu}}$
Gamma-Gamma, $(\mu,\nu),\eta$	$\sum_{k=0}^{\infty}\left(\zeta_k(\nu,\mu)\beta^{\frac{\nu+k}{2}-1}\right)+\sum_{k=0}^{\infty}\left(\zeta_k(\mu,\nu)\beta^{\frac{\mu+k}{2}-1}\right)$, where $\zeta_k(a,b)=\frac{\pi(ab)^{a+k}}{2(\eta)^{a+k}\sin((b-a)\pi)k!\Gamma(a)\Gamma(b)\Gamma(a-b+k+1)}$ if $\nu<\mu$ then $t_{gg}=\nu/2-1$ and $t_{gg}=\zeta_0(\nu,\mu)$ if $\nu>\mu$ then $t_{gg}=\mu/2-1$ and $t_{gg}=\zeta_0(\mu,\nu)$	t_{gg}	a_{gg}

TABLE II
VALUES OF PARAMETERS t AND a FOR DIFFERENT FADING CHANNELS

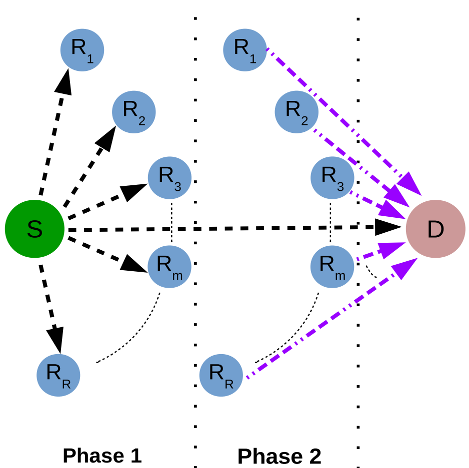

Fig. 1. Selective DF based $\mathcal{P}_0$ cooperative system with multiple relays.

independently with average gains of δ_{sd}^2, $\left(\delta_{sr}^{(r)}\right)^2$, $\left(\delta_{rd}^{(r)}\right)^2$, respectively. A novel aspect of the cooperative system model considered is that the various links may obey non-identical fading distributions, in contrast to [6]–[17], which consider identical fading distributions for the various constituent links. The circularly symmetric zero-mean complex additive white Gaussian noise at each receiving node has a variance of $\eta_0/2$ per dimension.

Let the average SNRs $\bar{\gamma}_{SD}$, $\bar{\gamma}_{SR}^{(r)}$, and $\bar{\gamma}_{RD}^{(r)}$ corresponding to the source-destination, source-relay r, and relay r-destination links be defined as, $\bar{\gamma}_{SD}=\frac{P_0}{\eta_0}$, $\bar{\gamma}_{SR}^{(r)}=\frac{P_0}{\eta_0}$, and $\bar{\gamma}_{RD}^{(r)}=\frac{P_r}{\eta_0}$, respectively. The instantaneous SNRs at the destination and relay r during the first phase and at the destination corresponding to the transmission by relay r at the end of the ensuing cooperative phase are given by:

$$\gamma_{SD}=\beta_{SD}\bar{\gamma}_{SD},\quad \gamma_{SR}^{(r)}=\beta_{SR}^{(r)}\bar{\gamma}_{SR}^{(r)},\quad \text{and}\quad \gamma_{RD}^{(r)}=\beta_{RD}^{(r)}\bar{\gamma}_{RD}^{(r)},$$

where $\beta_{SR}^{(r)}, \beta_{SD}$, and $\beta_{RD}^{(r)}$ are channel-dependent non-negative random variables. For instance, for the standard maximum ratio combining, we have $\beta=||\mathbf{h}||^2$, where $\mathbf{h}$ is the fading coefficient vector of the corresponding multiple-antenna link, while for MIMO scenarios associated with zero-forcing reception, $\beta=\frac{1}{N[(\mathbf{H}^H\mathbf{H})^{-1}]_{i,i}}$, where $\mathbf{H}$ denotes the MIMO channel matrix of the corresponding link, with N representing the number of transmitter antennas (TAs) and the subscript i denoting the i^{th} transmitted symbol. The variable β plays an important role in the proposed analysis and by appropriately choosing these parameters, one can analyze a wide variety of cooperative PHY layer schemes and fading channel distributions, as demonstrated in this treatise.

Since the high-SNR performance of the cooperative wireless system depends on the channel's probability density function (PDF) at $\beta \rightarrow 0^+$, we may invoke the following result, originally presented by Wang and Giannakis [19]. The PDF $f_\beta(\beta)$ of the quantity β corresponding to the various links can be approximated by a single polynomial term for $\beta \rightarrow 0^+$ as [19]

$$f_\beta(\beta)=a\beta^t+o\left(\beta^{t+\epsilon}\right), \tag{1}$$

where $\epsilon > 0$, $o\left(\beta^{t+\epsilon}\right)$ represents higher order terms, a is a positive constant and the parameter t characterizes the order of smoothness of the PDF $f_\beta(\beta)$ at the origin. The values of the parameters a and t can be determined using the PDF of the fading channel for single antenna nodes and are listed in Table II. However, for multiple antenna nodes, the values of these parameters depend also on the specific transmission/reception scheme employed in addition to the fading distribution(s), as it will be demonstrated in Section IV for various schemes such as zero-forcing, OSTBC etc. It is also worth mentioning that although the values of the parameters for Nakagami-m, Nakagami-q and Nakagami-n channels having unit average channel gains, i.e. $\delta^2 = 1$ and single TAs are given in [19], to the best of our knowledge, the values of these parameters for the other fading channels listed in Table II are not available in the open literature. Using the above framework, the following sub-section begins by deriving a general asymptotic upper bound on the end-to-end SER for the dual-phase protocol $\mathcal{P}_0$ described above, which is subsequently also employed for deriving both the diversity order and the optimal power fractions at the source and relays.

B. SER Analysis and Optimal Power Allocation of $\mathcal{P}_0$-based Selective DF Relaying

Let $\xi_j = [\xi_j(1), \xi_j(2), \cdots, \xi_j(R)]^T$ for $0 \le j \le 2^R - 1$ represent one of the possible 2^R network states, where $\xi_j(r)$ denotes the state of relay r for $1 \le r \le R$ that takes the binary values 1 and 0 corresponding to relay r decoding correctly and erroneously, respectively. For instance, ξ_0 represents the specific state in which all the relays decode in error, while on the other hand, ξ_{2^R-1} denotes the state in which all the relays decode the symbol transmitted by the source correctly. Based on this, the total end-to-end SER of the $\mathcal{P}_0$ cooperative system, conditioned on the channel state information (CSI), can be written as [16], [14]

$$\Pr(e|\underline{\beta}) = \sum_{j=0}^{2^R-1} \Pr(e|\xi_j, \underline{\beta}) \Pr(\xi_j|\underline{\beta}), \tag{2}$$

where $\underline{\beta} = \{\beta_{SD}, \beta_{SR}^{(r)}, \beta_{RD}^{(r)}, 1 \le r \le R\}$ depends on the CSI of the specific cooperative communication system. Furthermore, $\Pr(e|\xi_j, \underline{\beta})$ denotes the end-to-end SER conditioned on the cooperative system being in state ξ_j and the CSI $\underline{\beta}$, while $\Pr(\xi_j|\underline{\beta})$ denotes the corresponding probability of the system being in state ξ_j, conditioned on $\underline{\beta}$. Assuming the nodes of the cooperative system to be spatially distributed with independent and possibly non-identically fading links, the probability terms $\Pr(e|\xi_j, \underline{\beta})$, $\Pr(\xi_j|\underline{\beta})$ are independent, since the former depends on the SD and RD links, while the latter depends on the SR links. Averaging over the PDF of the CSI $\underline{\beta}$, the average end-to-end SER for the dual-phase protocol $\mathcal{P}_0$ is expressed as

$$\begin{aligned}\Pr(e) =& \mathbb{E}_{\underline{\beta}}\{\Pr(e|\underline{\beta})\} \\ =& \sum_{j=0}^{2^R-1} \mathbb{E}_{\underline{\beta}}\{\Pr(e|\xi_j, \underline{\beta}) \mathbb{E}_{\underline{\beta}}\{\Pr(\xi_j|\underline{\beta})\}.\end{aligned} \tag{3}$$

Let the set Ψ_j be defined as $\Psi_j = \{r|\xi_j(r) = 1, 1 \le r \le R\}$, i.e. Ψ_j includes all the relays that decode the symbol correctly. The result below represents the generalized asymptotic expression for the SER of the $\mathcal{P}_0$ protocol, which is applicable for various fading channels as well as PHY layer schemes, considering both M-PSK and M-QAM digital modulation schemes.

Theorem 1. *At high SNRs, the average end-to-end probability of symbol error Pr(e) at the destination node for the dual-phase protocol $\mathcal{P}_0$-based selective DF cooperative system is given by*

$$\begin{aligned}Pr(e) \doteq& \sum_{j=0}^{2^R-1} \frac{a_{SD}\Gamma(t_{SD}+1)}{(b_M \bar{\gamma}_{SD})^{t_{SD}+1}} C_{t_{SD}+1+\sum_{r\in\Psi_j} t_{RD}^{(r)} + |\Psi_j|} \\ &\times \prod_{r\in\Psi_j} \left\{ \frac{a_{RD}^{(r)} \Gamma\left(t_{RD}^{(r)}+1\right)}{\left(b_M \bar{\gamma}_{RD}^{(r)}\right)^{t_{RD}^{(r)}+1}} \right\} \\ &\times \prod_{r\in\bar{\Psi}_j} \left\{ \frac{a_{SR}^{(r)} \Gamma\left(t_{SR}^{(r)}+1\right)}{\left(b_M \bar{\gamma}_{SR}^{(r)}\right)^{t_{SR}^{(r)}+1}} \times C_{t_{SR}^{(r)}+1} \right\},\end{aligned} \tag{4}$$

where $\bar{\Psi}_j$ denotes the complement of the set Ψ_j and b_M is defined as

$$b_M = \begin{cases} \sin^2\left(\frac{\pi}{M}\right) & for\ M\text{–}PSK\ modulation, \\ \frac{3}{2(M-1)} & for\ M\text{–}QAM\ modulation. \end{cases} \tag{5}$$

The values of the constant C_n for the M-PSK and M-QAM modulation schemes are defined in equations (6) *and* (7) *respectively [2.511.2, [22]].*

Proof. Given in Appendix A. ∎

An illustrative application of the above result can be demonstrated for the simple case of the $\mathcal{P}_0$ protocol considering Rayleigh fading channels and QPSK modulation. For such a scenario, as shown in Table II, the parameters are $a_{SD} = \frac{1}{\delta_{SD}^2}, a_{RD}^{(r)} = \frac{1}{(\delta_{RD}^{(r)})^2}, a_{SR}^{(r)} = \frac{1}{(\delta_{SR}^{(r)})^2}, t_{SD} = t_{SR}^{(r)} = t_{RD}^{(r)} = 0$ in conjunction with $b_4 = \sin^2(\frac{\pi}{4}) = \frac{1}{2}$ corresponding to QPSK modulation. Substituting the above quantities into Eq. (4), the resultant $\Pr(e)$ at high SNRs at the destination node is given by

$$\begin{aligned}\Pr(e) \doteq& \sum_{j=0}^{2^R-1} \frac{2^{|\Psi_j|+|\bar{\Psi}_j|+1} C_{|\Psi_j|+1}}{\delta_{SD}^2 \bar{\gamma}_{SD}} \prod_{r\in\Psi_j} \left\{ \frac{1}{\left(\delta_{RD}^{(r)}\right)^2 \bar{\gamma}_{RD}^{(r)}} \right\} \\ &\times \prod_{r\in\bar{\Psi}_j} \left\{ \frac{C_1}{\left(\delta_{SR}^{(r)}\right)^2 \bar{\gamma}_{SR}^{(r)}} \right\}.\end{aligned} \tag{8}$$

Similarly, the corresponding SER results can now be derived for several other fading channels listed in Table II in a straightforward fashion, which demonstrates the wide applicability of the above framework. The diversity order and the optimal power allocation of the $\mathcal{P}_0$ protocol are developed next.

$$C_n=\frac{1}{\pi}\int_0^{\frac{(M-1)\pi}{M}}\sin^{2n}\theta d\theta=-\frac{\cos\left(\frac{(M-1)\pi}{M}\right)}{2n\pi}\left\{\sin^{2n-1}\left(\frac{(M-1)\pi}{M}\right)+\sum_{k=1}^{n-1}\frac{(2n-1)(2n-3)\cdots(2n-2k+1)}{2^k(n-1)(n-2)\cdots(n-k)}\right.$$
$$\left.\times\sin^{2n-2k-1}\left(\frac{(M-1)\pi}{M}\right)\right\}+\frac{(2n-1)(2n-3)\cdots 1(M-1)}{2^n n!M}. \quad (6)$$

$$C_n=\frac{4}{\pi\sqrt{M}}\left(1-\frac{1}{\sqrt{M}}\right)\int_0^{\frac{\pi}{2}}\sin^{2n}\theta d\theta+\frac{4}{\pi}\left(1-\frac{1}{\sqrt{M}}\right)^2\int_{\frac{\pi}{4}}^{\frac{\pi}{2}}\sin^{2n}\theta d\theta$$
$$=\frac{1}{n\pi}\left(1-\frac{1}{\sqrt{M}}\right)^2\left(\frac{1}{2}\right)^{n-1}\left\{1+\sum_{k=1}^{n-1}\frac{(2n-1)(2n-3)\cdots(2n-2k+1)}{(n-1)(n-2)\cdots(n-k)}\right\}$$
$$+\frac{(2n-1)(2n-3)\cdots 1(M-1)}{2^n n!M}. \quad (7)$$

1) Diversity Order and Optimal Power Allocation for the $\mathcal{P}_0$ Selective DF Multiple Relay System: Let the power fractions for the source and r^{th} relay, denoted by α_0,α_r respectively, be defined as $\alpha_0=P_0/P,\alpha_r=P_r/P,1\le r\le R$. Substituting $\bar{\gamma}_{SD}=\bar{\gamma}_{SR}^{(r)}=\frac{\alpha_0 P}{\eta_0}$ and $\bar{\gamma}_{RD}^{(r)}=\frac{\alpha_r P}{\eta_0}$ into the expression for the end-to-end SER Pr(e) derived in Theorem 1 yields

$$\Pr(e)\doteq\sum_{j=0}^{2^R-1}\frac{\mathcal{C}_j\left(\eta_0/P\right)^{d_j}}{\left(\alpha_0\right)^{t_{SD}+1+\sum_{r\in\bar{\Psi}_j}t_{SR}^{(r)}+|\bar{\Psi}_j|}\prod_{r\in\Psi_j}(\alpha_r)^{t_{RD}^{(r)}+1}}, \quad (9)$$

where the exponent d_j and the constant $\mathcal{C}_j$ corresponding to the state ξ_j are given as

$$d_j=t_{SD}+\sum_{r\in\Psi_j}t_{RD}^{(r)}+\sum_{r\in\bar{\Psi}_j}t_{SR}^{(r)}+R+1, \quad (10)$$
$$\mathcal{C}_j=\frac{a_{SD}\Gamma(t_{SD}+1)C_{t_{SD}+1+\sum_{r\in\Psi_j}t_{RD}^{(r)}+|\Psi_j|}}{(b_M)^{t_{SD}+\sum_{r\in\Psi_j}t_{RD}^{(r)}+\sum_{r\in\bar{\Psi}_j}t_{SR}^{(r)}+R+1}}\prod_{r\in\Psi_j}\left\{a_{RD}^{(r)}\right.$$
$$\left.\times\Gamma\left(t_{RD}^{(r)}+1\right)\right\}\prod_{r\in\bar{\Psi}_j}\left\{a_{SR}^{(r)}\Gamma\left(t_{SR}^{(r)}+1\right)C_{t_{SR}^{(r)}+1}\right\}. \quad (11)$$

The optimal power fractions and hence the optimal source-relay power sharing is now given by the result below.

Theorem 2. *The optimal power fractions $\alpha_0,\alpha_r,1\le r\le R$, for the dual-phase protocol $\mathcal{P}_0$-based selective DF cooperative system relying on R relays are given by the solution of the optimization problem below*

$$\min_{\alpha_0,\alpha_1,\ldots,\alpha_R}\sum_{j=0}^{2^R-1}\frac{\mathcal{C}_j(\eta_0/P)^{d_j}}{(\alpha_0)^{t_{SD}+1+\sum_{r\in\bar{\Psi}_j}t_{SR}^{(r)}+|\bar{\Psi}_j|}\prod_{r\in\Psi_j}(\alpha_r)^{t_{RD}^{(r)}+1}},$$
$$\textit{s.t.}\quad \alpha_0+\sum_{r=1}^{R}\alpha_r=1,\alpha_0\ge 0,\alpha_r\ge 0,1\le r\le R, \quad (12)$$

where the quantities d_j and $\mathcal{C}_j$ are defined in (10) *and* (11)*, respectively.*

Proof. The optimization problem above can be readily formulated by minimizing the value of Pr(e) from (9) together with the total power budget of the $\mathcal{P}_0$ protocol limited by P, leading to the constraint in (12) in terms of the power fractions α_0,α_r. ■

It can be seen that the optimization problem in (12) is a standard geometric program (GP) [23] that can be solved to obtain the optimal source-relay power fractions for a multi-relay scenario using a convex solver such as CVX [24]. Moreover, one can also explicitly obtain the optimal power fractions for a single relay scenario, i.e. for $R=1$ as given by the following result.

Lemma 1. *The optimal power fractions α_0,α_1 for a $R=1$ relay $\mathcal{P}_0$ protocol, with $t_{SD}=t_{SR}=t_{RD}=0$ that holds for various fading channels such as Rayleigh, Nakagami-q, Nakagami-n, Rician, and Shadowed Rician as shown in Table II, are obtained as*

$$\alpha_0=\frac{\tilde{c}_2-2\pm\sqrt{4\tilde{c}_1-3\tilde{c}_2}}{2(\tilde{c}_1-1)},\alpha_1=\frac{2\tilde{c}_1-\tilde{c}_2\mp\sqrt{4\tilde{c}_1-3\tilde{c}_2}}{2(\tilde{c}_1-1)}, \quad (13)$$

where the constants are $\tilde{c}_1=\frac{C_2 a_{RD}}{C_1^2 a_{SR}}$ and $\tilde{c}_2=\frac{C_2 a_{RD}}{2C_1^2 a_{SR}}$.

Proof. For $R=1$, the optimization problem in (12) reduces to

$$\min_{\alpha_0,\alpha_1}\left[\frac{\tau_1}{(\alpha_0)^{t_{SD}+t_{SR}+2}}+\frac{\tau_2}{(\alpha_0)^{t_{SD}+1}(\alpha_1)^{t_{RD}+1}}\right],$$
$$\text{s.t.}\quad \alpha_0+\alpha_1=1, \quad (14)$$

where the constants τ_1 and τ_2 are defined as

$$\tau_1=\frac{a_{SD}\Gamma(t_{SD}+1)C_{t_{SD}+1}a_{SR}\Gamma(t_{SR}+1)C_{t_{SR}+1}}{(b_M P/\eta_0)^{t_{SD}+t_{SR}+2}},$$
$$\tau_2=\frac{a_{SD}\Gamma(t_{SD}+1)C_{t_{SD}+t_{RD}+2}a_{RD}\Gamma(t_{RD}+1)}{(b_M P/\eta_0)^{t_{SD}+t_{RD}+2}}. \quad (15)$$

The optimization problem given in (14) can now be solved using the Karush-Kuhn-Tucker (KKT) framework, i.e. by differentiating it with respect to α_0 and then setting it equal to zero, which yields the following polynomial equation for α_0

$$-(1-\alpha_0)^{t_{RD}+2}+\tilde{c}_1\alpha_0^{t_{SR}+2}-\tilde{c}_2\alpha_0^{t_{SR}+1}=0, \qquad (16)$$

where the constants $\tilde{c}_1=\frac{\tau_2}{\tau_1}$ and $\tilde{c}_2=\frac{(t_{SD}+1)\tau_2}{(t_{SD}+t_{SR}+2)\tau_1}$. A non-negative zero of the above polynomial equation yields the optimal power fraction α_0^*, $0<\alpha_0^*\leq 1$ at the source and therefore, the optimal power fraction for the relay is $\alpha_1^*=1-\alpha_0^*$. Furthermore, setting $t_{SD}=t_{SR}=t_{RD}=0$ for the various fading channels considered in Lemma 1, the roots of the resultant quadratic equation for α_0 can be evaluated as shown in (13). ■

The generalized expression for the diversity order of the $\mathcal{P}_0$ protocol and its impact on the optimal power sharing for various scenarios is described next. Since the term corresponding to the minimum value of the exponent d_j dominates the end-to-end SER expression of (9) at high SNRs, the diversity order is given by

$$\begin{aligned} d_{\mathcal{P}_0}&=\min_{0\leq j\leq 2^R-1} d_j \\ &=t_{SD}+R+1+\min_{0\leq j\leq 2^R-1}\left\{\sum_{r\in\Psi_j}t_{RD}^{(r)}+\sum_{r\in\bar{\Psi}_j}t_{SR}^{(r)}\right\}. \end{aligned} \qquad (17)$$

In order to gain deeper insights into the diversity order and optimal power sharing, consider $t_{SR}^{(r)}=t_{SR}$ and $t_{RD}^{(r)}=t_{RD}$ for $1\leq r\leq R$. For this scenario, the expression in (9) can be simplified as

$$\begin{aligned} \Pr(e)\doteq&\sum_{j=0}^{2^R-1}\left[\frac{\widetilde{\mathcal{C}}_j}{(\alpha_0)^{t_{SD}+1+t_{SR}|\bar{\Psi}_j|+|\bar{\Psi}_j|}\prod\limits_{r\in\Psi_j}(\alpha_r)^{t_{RD}+1}}\right] \\ &\times\left(\frac{\eta_0}{P}\right)^{\overbrace{t_{SD}+t_{RD}|\Psi_j|+t_{SR}|\bar{\Psi}_j|+R+1}^{\mathcal{D}_j}}, \end{aligned} \qquad (18)$$

where the constant $\widetilde{\mathcal{C}}_j$ is defined as

$$\begin{aligned} \widetilde{\mathcal{C}}_j=&\frac{a_{SD}\Gamma(t_{SD}+1)C_{t_{SD}+1+t_{RD}|\Psi_j|+|\Psi_j|}}{(b_M)^{t_{SD}+t_{RD}|\Psi_j|+t_{SR}|\bar{\Psi}_j|+R+1}}\prod_{r\in\Psi_j}\left\{a_{RD}^{(r)}\Gamma(t_{RD}+1)\right\} \\ &\times\prod_{r\in\bar{\Psi}_j}\left\{a_{SR}^{(r)}\Gamma\left(t_{SR}+1\right)C_{t_{SR}+1}\right\}. \end{aligned} \qquad (19)$$

Therefore, the diversity order is seen to be given as

$$\begin{aligned} d_{\mathcal{P}_0}&=\min_j\ \mathcal{D}_j \\ &=t_{SD}+R+1+\min_j\left\{t_{RD}|\Psi_j|+t_{SR}|\bar{\Psi}_j|\right\} \\ &=t_{SD}+R+1+\min_j\left\{t_{RD}|\Psi_j|+t_{SR}(R-|\Psi_j|)\right\} \\ &=t_{SD}+R+1+t_{SR}R+\min_j\left\{(t_{RD}-t_{SR})|\Psi_j|\right\}. \end{aligned} \qquad (20)$$

The results below give the simplified SER expressions for various scenarios that are seen to yield important insights.

Lemma 2. *For the scenario having diversity orders higher than those of the source-relay links for the relay-destination links, i.e. for $t_{RD}+1>t_{SR}+1\Rightarrow t_{RD}>t_{SR}$, the end-to-end SER for the dual-phase protocol $\mathcal{P}_0$-based selective DF cooperative system can be simplified to*

$$\begin{aligned} Pr(e)\doteq&\frac{a_{SD}\Gamma(t_{SD}+1)C_{t_{SD}+1}}{(b_M\alpha_0)^{t_{SD}+1+t_{SR}R+R}}\prod_{r=1}^{R}\left\{a_{SR}^{(r)}\Gamma\left(t_{SR}+1\right)\right. \\ &\left.\times C_{t_{SR}+1}\right\}\left(\frac{\eta_0}{P}\right)^{t_{SD}+t_{SR}R+R+1}, \end{aligned} \qquad (21)$$

with the corresponding diversity order for this scenario obtained as $t_{SD}+t_{SR}R+R+1$.

Proof. For the scenario when $t_{RD}>t_{SR}$, it can be seen that $\min\limits_j\left\{(t_{RD}-t_{SR})|\Psi_j|\right\}=0$ when $|\Psi_j|=0$. Hence the dominant term in (18) corresponds to the state $\xi_0=[0,0,\cdots,0]^T$, with each relay in the multiple-relay system decoding in error. Therefore, neglecting the terms $j\neq 0$, and substituting $|\Psi_j|=0,|\bar{\Psi}_j|=R$ into (18) yields the end-to-end SER as

$$\begin{aligned} \Pr(e)\doteq&\frac{a_{SD}\Gamma(t_{SD}+1)\zeta(t_{SD}+1)}{(b_M\alpha_0)^{t_{SD}+1+t_{SR}R+R}}\prod_{r=1}^{R}\left\{a_{SR}^{(r)}\Gamma\left(t_{SR}+1\right)\right. \\ &\left.\times\zeta\left(t_{SR}+1\right)\right\}\left(\frac{\eta_0}{P}\right)^{t_{SD}+t_{SR}R+R+1}. \end{aligned} \qquad (22)$$

Furthermore, from the exponent of the $1/\text{SNR}$ term (η_0/P) from above, it can be seen that the diversity order is $t_{SD}+t_{SR}R+R+1$. ■

Moreover, it is seen from the above result that the end-to-end SER performance of the system for this scenario of $t_{RD}>t_{SR}$ depends only on the source power fraction α_0. Hence, the end-to-end error $\Pr(e)$ is minimized by setting α_0 close to its maximum possible value, i.e. to 1. In other words, P_0 is approximately P, which in turn implies that a significant portion of the available power is allocated to the source.

Lemma 3. *For the scenario with the diversity orders higher than those of the relay-destination links for the source-relay links, i.e. $t_{RD}+1<t_{SR}+1\Rightarrow t_{RD}<t_{SR}$, the end-to-end SER for the dual-phase protocol $\mathcal{P}_0$-based selective DF cooperative system is obtained as*

$$\begin{aligned} Pr(e)\doteq&\frac{a_{SD}\Gamma(t_{SD}+1)}{(b_M\alpha_0)^{t_{SD}+1}}\prod_{r=1}^{R}\left\{\frac{a_{RD}^{(r)}\Gamma\left(t_{RD}+1\right)}{(b_M\alpha_r)^{t_{RD}+1}}\right\} \\ &\times C_{t_{SD}+1+t_{RD}R+R}\left(\frac{\eta_0}{P}\right)^{t_{SD}+t_{RD}R+R+1}, \end{aligned} \qquad (23)$$

with the corresponding diversity order for this scenario determined as $t_{SD}+t_{RD}R+R+1$.

Proof. The proof is similar to that of Lemma 2 above and can be derived by noting that when $t_{RD}<t_{SR}$, we have $\min\limits_j\left\{(t_{RD}-t_{SR})|\Psi_j|\right\}=(t_{RD}-t_{SR})R$ corresponding to the state $\xi_{2^R-1}=[1,1,\cdots,1]^T$ with $|\Psi_{2^R-1}|=R$. Retaining only the dominant term $j=2^R-1$ and ignoring the rest leads to the result above. ■

Furthermore, with respect to the power sharing for this scenario, it is seen that error rate minimization corresponds to maximizing the product $\alpha_0\prod_{r=1}^{R}\alpha_r$ in (23). This is in turn achieved by setting $\alpha_0=\alpha_r=\frac{1}{R+1}, 1\leq r\leq R$, corresponding to equal power sharing between the source and the relays.

Finally, for the scenario of $t_{SR} = t_{RD}$, all the terms corresponding to the states $\xi_j, 0 \leq j \leq 2^R - 1$ contribute to (18). It can be seen from (20) that the diversity order achieved for this scenario is $t_{SD} + t_{SR}R + R + 1$, since $t_{SR} - t_{RD} = 0$. Therefore, this result and the ones in Lemmas 2, 3 can now be combined to yield the general expression for the diversity order of

$$d_{\mathcal{P}_0} = t_{SD} + 1 + R(\min\{t_{SR}, t_{RD}\} + 1). \tag{24}$$

As a simple illustration, setting $t_{SR} = t_{RD} = t_{SD} = 0$ corresponding to various fading channels such as Rayleigh, Rician, Nakagam-q etc. with single antenna nodes yields the standard result of $d_{\mathcal{P}_0} = R + 1$. The framework for the asymptotic performance analysis of the class of $\mathcal{P}_m, 1 \leq m < R$ selective DF multi-relay multi-phase cooperative protocols is detailed next.

III. $\mathcal{P}_m$ BASED SELECTIVE DF RELAYING

A. System Model

Consider the multi-phase relaying protocol $\mathcal{P}_m$ as shown in Fig. 2, which, in contrast to the dual-phase cooperative protocol $\mathcal{P}_0$, allows inter-relay communication between the relays. The channels between the various relay pairs $\tilde{r}$ and r are assumed to be fading independently with average gains of $\left(\delta_{rr}^{(r,\tilde{r})}\right)^2$. Therefore, the instantaneous SNR corresponding to the transmission between relay $\tilde{r}$ and relay r can be expressed as, $\gamma_{RR}^{(r,\tilde{r})} = \beta_{RR}^{(r,\tilde{r})}\bar{\gamma}_{RR}^{(r,\tilde{r})}$ where $\beta_{RR}^{(r,\tilde{r})}$ is a channel fading distribution dependent non-negative random parameter and the SNR constant $\bar{\gamma}_{RR}^{(r,\tilde{r})}$ is defined as $\bar{\gamma}_{RR}^{(r,\tilde{r})} = \frac{P_r}{\eta_0}$. In the $\mathcal{P}_m$ protocol, the cooperative relaying transmissions are spread over a total duration of $R + 1$ phases with each relay receiving the signal from the source and at most m previous relays. The source transmits the symbol in the first phase, while each individual relay r selectively retransmits in phase $r + 1$, after combining the transmission of the source with the signals received from $\min\{m, r - 1\}$ previous relay transmissions. Finally, the destination decodes the symbol after $R + 1$ communication phases using the signals received from the source and the relays.

B. SER Analysis and Optimal Power Allocation of $\mathcal{P}_m$ based Selective DF Relaying

Similar to the analysis for the $\mathcal{P}_0$ cooperative protocol in Section II-B, let the state of relay r and the network state be defined as $\xi_j(r)$ and ξ_j, respectively. Furthermore, let $\Psi_j(r)$ be defined as, $\Psi_j(r) = \{\tilde{r} | \max\{1, r - m\} \leq \tilde{r} < r, \xi_j(\tilde{r}) = 1\}$, i.e. all the relays preceding relay r which decode the symbol transmitted by the source correctly. Below we derive a generalized high-SNR end-to-end SER expression for the $\mathcal{P}_m$ protocol.

Theorem 3. *At high SNRs, the average end-to-end probability of symbol error $Pr(e)$ at the destination for a $\mathcal{P}_m$ based selective DF multi-relay cooperative system is given by*

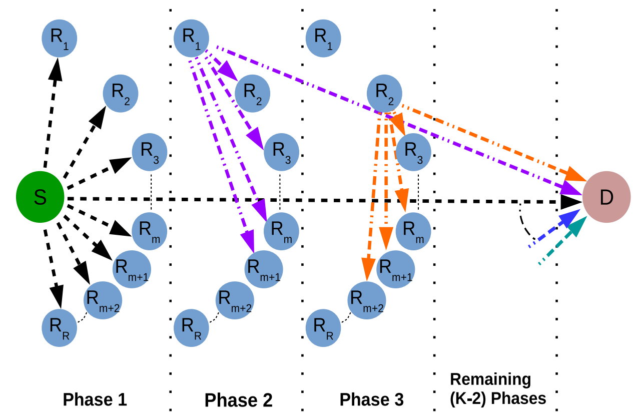

Fig. 2. Selective DF based $\mathcal{P}_m$ cooperative system with multiple relays.

$$\begin{aligned} Pr(e) \doteq & \sum_{j=0}^{2^R-1} \frac{a_{SD}\Gamma(t_{SD}+1)}{(b_M\bar{\gamma}_{SD})^{t_{SD}+1}} C_{t_{SD}+1+\sum_{r\in\Psi_j} t_{RD}^{(r)}+|\Psi_j|} \\ & \times \prod_{r\in\Psi_j} \left\{ \frac{a_{RD}^{(r)}\Gamma\left(t_{RD}^{(r)}+1\right)}{(b_M\bar{\gamma}_{RD}^{(r)})^{t_{RD}^{(r)}+1}} \right\} \\ & \times \prod_{r\in\bar{\Psi}_j} \left\{ \frac{a_{SR}^{(r)}\Gamma(t_{SR}^{(r)}+1)}{(b_M\bar{\gamma}_{SR}^{(r)})^{t_{SR}^{(r)}+1}} \prod_{q\in\Psi_j(r)} \left\{ \frac{a_{RR}^{(q,r)}\Gamma(t_{RR}^{(q,r)}+1)}{(b_M\bar{\gamma}_{RR}^{(q,r)})^{t_{RR}^{(q,r)}+1}} \right\} \right. \\ & \left. \times C_{t_{SR}^{(r)}+1+\sum_{q\in\Psi_j(r)}\left(t_{RR}^{(q,r)}+1\right)} \right\}, \end{aligned} \tag{25}$$

where the constants b_M and C_n are as defined in Theorem 1.

Proof. Given in Appendix D. ∎

To illustrate the applicability of the above result, one can derive the end-to-end SER at the destination for the multi-phase protocol $\mathcal{P}_m$-based system using M-ary PSK over a standard Rayleigh fading channel by setting the parameters as $a_{SD} = \frac{1}{\delta_{SD}^2}, a_{RD}^{(r)} = \frac{1}{(\delta_{RD}^{(r)})^2}, a_{SR}^{(r)} = \frac{1}{(\delta_{SR}^{(r)})^2}, a_{RR}^{(q,r)} = \frac{1}{(\delta_{RR}^{(q,r)})^2}, t_{SD} = t_{SR}^{(r)} = t_{RD}^{(r)} = t_{RR}^{(q,r)} = 0$ with $b_M = \sin^2(\pi/M)$ in Eq. (25) above. The corresponding closed-form expression for $\Pr(e)$ of the system is obtained as

$$\begin{aligned} \Pr(e) \doteq & \sum_{j=0}^{2^R-1} \frac{C_{|\Psi_j|+1}}{b_M\delta_{SD}^2\bar{\gamma}_{SD}} \prod_{r\in\Psi_j} \left\{ \frac{1}{b_M(\delta_{RD}^{(r)})^2\bar{\gamma}_{RD}^{(r)}} \right\} \\ & \times \prod_{r\in\bar{\Psi}_j} \left\{ \frac{C_{|\Psi_j(r)|+1}}{b_M(\delta_{SR}^{(r)})^2\bar{\gamma}_{SR}^{(r)}} \prod_{q\in\Psi_j(r)} \left\{ \frac{1}{b_M(\delta_{RR}^{(q,r)})^2\bar{\gamma}_{RR}^{(q,r)}} \right\} \right\}. \end{aligned} \tag{26}$$

The next subsection characterizes the optimal source relay power sharing and diversity order for the $\mathcal{P}_m$ protocol.

1) Diversity Order and Optimal Source Relay Power Allocation For $\mathcal{P}_m$ based Cooperative Communication: Employing the power fractions $\alpha_0 = P_0/P, \alpha_r = P_r/P, 1 \leq r \leq R$, the expression in (25) above for the end-to-end SER of the

$\mathcal{P}_m$ system can be recast as

$$\Pr(e) \doteq \sum_{j=0}^{2^R-1} \frac{X_j}{(\alpha_0)^{t_{SD}+1+\sum_{r\in\bar{\Psi}_j} t_{SR}^{(r)}+|\bar{\Psi}_j|} \prod_{r\in\Psi_j}(\alpha_r)^{t_{RD}^{(r)}+1}} \times \frac{1}{\prod_{r\in\bar{\Psi}_j}\prod_{q\in\Psi_j(r)}(\alpha_q)^{t_{RR}^{(q,r)}+1}} \left(\frac{\eta_0}{P}\right)^{d_j}, \quad (27)$$

where $d_j = t_{SD} + R + 1 + \sum_{r\in\Psi_j} t_{RD}^{(r)} + \sum_{r\in\bar{\Psi}_j} t_{SR}^{(r)} + \sum_{r\in\bar{\Psi}_j}\sum_{q\in\Psi_j(r)} \left(t_{RR}^{(q,r)}+1\right)$ and the coefficient X_j corresponding to state ξ_j is defined as

$$X_j = \frac{a_{SD}\Gamma(t_{SD}+1)}{(b_M)^{t_{SD}+1}} C_{t_{SD}+1+\sum_{r\in\Psi_j} t_{RD}^{(r)}+|\Psi_j|} \times \prod_{r\in\Psi_j}\left\{\frac{a_{RD}^{(r)}\Gamma\left(t_{RD}^{(r)}+1\right)}{(b_M)^{t_{RD}^{(r)}+1}}\right\} \times \prod_{r\in\bar{\Psi}_j}\left\{\frac{a_{SR}^{(r)}\Gamma(t_{SR}^{(r)}+1)}{(b_M)^{t_{SR}^{(r)}+1}} \prod_{q\in\Psi_j(r)}\left\{\frac{a_{RR}^{(q,r)}\Gamma(t_{RR}^{(q,r)}+1)}{(b_M)^{t_{RR}^{(q,r)}+1}}\right\} \times C_{t_{SR}^{(r)}+1+\sum_{q\in\Psi_j(r)}\left(t_{RR}^{(q,r)}+1\right)}\right\}. \quad (28)$$

It can be observed that the exponent d_j can be lower-bounded as $d_j \geq t_{SD} + R + 1 + \sum_{r\in\Psi_j} t_{RD}^{(r)} + \sum_{r\in\bar{\Psi}_j} t_{SR}^{(r)}$ with equality when $\sum_{r\in\bar{\Psi}_j}\sum_{q\in\Psi_j(r)}\left(t_{RR}^{(q,r)}+1\right) = 0$, i.e. $|\Psi_j(r)| = 0, \forall r \in \bar{\Psi}_j$, which arises for the states, $\xi_{2^R-1} = [1,1,1,\cdots 1]^T$, $\xi_{2^{R-1}-1} = [0,1,1,\cdots 1]^T$, $\xi_{2^{R-2}-1} = [0,0,1,\cdots 1]^T$, $\cdots$, $\xi_0 = [0,0,0,\cdots 0]^T$. Hence, considering the dominant $(R+1)$ terms in the expression of $\Pr(e)$ corresponding to the above states, the convex optimization problem for optimal source-relay power allocation in the $\mathcal{P}_m$ protocol can be formulated as

$$\min_{\alpha_0,\alpha_1,\ldots,\alpha_R} \sum_{\substack{k=0,\\ j=2^k-1}}^{R} \frac{X_j(\eta_0/P)^{d_j}}{(\alpha_0)^{t_{SD}+1+\sum_{r\in\bar{\Psi}_j} t_{SR}^{(r)}+|\bar{\Psi}_j|} \prod_{r\in\Psi_j}(\alpha_r)^{t_{RD}^{(r)}+1}},$$
$$\text{s.t.} \quad \alpha_0 + \sum_{r=1}^{R}\alpha_r = 1, \alpha_0 \geq 0, \alpha_r \geq 0, 1 \leq r \leq R, \quad (29)$$

where $d_j = t_{SD} + R + 1 + \sum_{r\in\Psi_j} t_{RD}^{(r)} + \sum_{r\in\bar{\Psi}_j} t_{SR}^{(r)}$ and the constant term X_j is defined as

$$X_j = \frac{a_{SD}\Gamma(t_{SD}+1)}{(b_M)^{t_{SD}+1}} C_{t_{SD}+1+\sum_{r\in\Psi_j} t_{RD}^{(r)}+|\Psi_j|} \prod_{r\in\Psi_j}\left\{\frac{a_{RD}^{(r)}}{(b_M)^{t_{RD}^{(r)}+1}} \times\Gamma\left(t_{RD}^{(r)}+1\right)\right\} \prod_{r\in\bar{\Psi}_j}\left\{\frac{a_{SR}^{(r)}\Gamma(t_{SR}^{(r)}+1)}{(b_M)^{t_{SR}^{(r)}+1}} C_{t_{SR}^{(r)}+1}\right\}. \quad (30)$$

The associated diversity order is $d = \min_{j=2^k-1, 0\leq k\leq R} d_j = t_{SD} + R + 1 + \min_{j=2^k-1,0\leq k\leq R}\left\{\sum_{r\in\Psi_j} t_{RD}^{(r)} + \sum_{r\in\bar{\Psi}_j} t_{SR}^{(r)}\right\}$. Interesting insights can now be obtained both for the diversity order and for the optimal power sharing by considering $t_{SR}^{(r)} = t_{SR}$ and $t_{RD}^{(r)} = t_{RD}$, $\forall r$. For such a scenario, considering only the dominant $(R+1)$ terms described above, the expression in Eq. (27) for the average SER reduces to

$$\Pr(e) \doteq \sum_{\substack{k=0,\\ j=2^k-1}}^{R} \mathcal{X}_j \left(\frac{\eta_0}{P}\right)^{\mathcal{D}_j}, \quad (31)$$

where the exponent $\mathcal{D}_j$ and the coefficient $\mathcal{X}_j$ are defined as

$$\mathcal{D}_j = t_{SD} + R + 1 + Rt_{RD} + |\bar{\Psi}_j|(t_{SR} - t_{RD}), \quad (32)$$
$$\mathcal{X}_j = \frac{a_{SD}\Gamma(t_{SD}+1)}{(b_M\alpha_0)^{t_{SD}+1}} C_{t_{SD}+1+(t_{RD}+1)(R-|\bar{\Psi}_j|)} \times \prod_{r=|\bar{\Psi}_j|+1}^{R}\left\{\frac{a_{RD}^{(r)}\Gamma(t_{RD}+1)}{(b_M\alpha_r)^{t_{RD}+1}}\right\} \times \prod_{r=1}^{|\bar{\Psi}_j|}\left\{\frac{a_{SR}^{(r)}\Gamma(t_{SR}+1)}{(b_M\alpha_0)^{t_{SR}+1}} C_{t_{SR}+1}\right\}. \quad (33)$$

Furthermore, by setting $t_{SR}^{(r)} = t_{SR}$ and $t_{RD}^{(r)} = t_{RD}$, $\forall r$, it follows from (32) that the diversity order achieved is

$$d = \min_{j=2^k-1,0\leq k\leq R} \mathcal{D}_j = t_{SD}+R+1+Rt_{RD}+\min_{j=2^k-1,0\leq k\leq R}\{|\bar{\Psi}_j|(t_{SR}-t_{RD})\}. \quad (34)$$

Based on the above result, the end-to-end SER and diversity order expressions of the $\mathcal{P}_m$ protocol in various scenarios are derived next.

Lemma 4. *The end-to-end SERs for $t_{SR} > t_{RD}$ and $t_{SR} < t_{RD}$ respectively at high SNRs in the $\mathcal{P}_m$ cooperative system are given as*

$$Pr(e)|_{t_{SR}>t_{RD}} \doteq \frac{a_{SD}\Gamma(t_{SD}+1)}{(b_M\alpha_0)^{t_{SD}+1}} C_{t_{SD}+1+(t_{RD}+1)R} \times \prod_{r=1}^{R}\left\{\frac{a_{RD}^{(r)}\Gamma(t_{RD}+1)}{(b_M\alpha_r)^{t_{RD}+1}}\right\}\left(\frac{\eta_0}{P}\right)^{t_{SD}+1+Rt_{RD}+R}, \quad (35)$$

$$Pr(e)|_{t_{SR}<t_{RD}} \doteq \frac{a_{SD}\Gamma(t_{SD}+1)}{(b_M\alpha_0)^{t_{SD}+1}} C_{t_{SD}+1} \times \prod_{r=1}^{R}\left\{\frac{a_{SR}^{(r)}\Gamma(t_{SR}+1)}{(b_M\alpha_0)^{t_{SR}+1}} C_{t_{SR}+1}\right\}\left(\frac{\eta_0}{P}\right)^{t_{SD}+1+Rt_{SR}+R}, \quad (36)$$

and the corresponding diversity orders are

$$d|_{t_{SR}>t_{RD}} = t_{SD} + 1 + Rt_{RD} + R, \quad (37)$$
$$d|_{t_{SR}<t_{RD}} = t_{SD} + 1 + Rt_{SR} + R. \quad (38)$$

Proof. The proof follows from the fact that for $t_{SR} > t_{RD}$, $\min_{j=2^k-1,0\leq k\leq R}\{|\bar{\Psi}_j|(t_{SR} - t_{RD})\} = 0$ occurs when $|\bar{\Psi}_j|$ is minimum, which in turn occurs for the state $\xi_{j=2^R-1} = [1,1,\cdots,1]^T$, i.e. when none of the R relays decode erroneously. Hence, considering the dominant term corresponding to $\xi_{j=2^R-1}$ in the SER expression (31) and neglecting all other terms yields the end-to-end SER approximation in (35) and the diversity order is seen to be $(t_{SD}+1+Rt_{RD}+R)$ from the exponent of the quantity (η_0/P). The analogous result for $t_{SR} < t_{RD}$ is similarly derived by noting that the dominant term in the $\Pr(e)$ expression in (31) for this case corresponds to the state $\xi_{j=0} = [0,0,\cdots,0]^T$ in which $\min\{|\bar{\Psi}_j|(t_{SR}-t_{RD})\} = -R$ occurs when $|\bar{\Psi}_j| = R$. ■

Furthermore, for the scenario of $t_{SR} = t_{RD}$, the diversity order can be seen from (31) to be $(t_{SD}+1+Rt_{RD}+R)$. Finally, by considering the minimum of the diversity orders obtained for the scenarios of $t_{SR} = t_{RD}$, $t_{SR} > t_{RD}$, and $t_{SR} < t_{RD}$, a succinct expression for the diversity order of this system can be derived as

$$d_{\mathcal{P}_m} = t_{SD}+1+R(\min\{t_{SR},t_{RD}\}+1). \tag{39}$$

Considering now the aspect of optimal power sharing, when $t_{SR} > t_{RD}$, it can seen from (35) that all the power fractions $\alpha_0, \alpha_r, 1 \le r \le R$ contribute to the end-to-end $\Pr(e)$. Hence, the optimal power sharing is given as $\alpha_0 = \alpha_r = \frac{1}{R+1}, 1 \le r \le R$, i.e. equal power sharing across all the transmitting nodes is optimal. On the other hand, for $t_{SR} < t_{RD}$, $\alpha_0 = 1$ is optimal since only the power fraction α_0 is present in the dominant terms in the expression for $\Pr(e)$ in (36). For a general scenario, the pertinent optimization problem for source-relay power utilization in the $\mathcal{P}_m$ system, considering $t_{SR}^{(r)} = t_{SR}$ and $t_{RD}^{(r)} = t_{RD}, \forall r$ can be formulated as

$$\begin{aligned}\min_{\alpha_0,\alpha_1,\ldots,\alpha_R} \quad & \sum_{\substack{k=0,\\ j=2^k-1}}^{R} \frac{\widetilde{X}_j}{\alpha_0^{t_{SD}+1+|\bar{\Psi}_j|(t_{SR}+1)} \prod_{r=|\bar{\Psi}_j|+1}^{R} \alpha_r^{t_{RD}+1}},\\ \text{s.t.} \quad & \alpha_0 + \sum_{r=1}^{R}\alpha_r = 1,\\ & \alpha_0 \ge 0, \alpha_r \ge 0, 1 \le r \le R,\end{aligned} \tag{40}$$

where the coefficient $\widetilde{X}_j$ corresponding to state j is defined as

$$\begin{aligned}\widetilde{X}_j =& \frac{a_{SD}\Gamma(t_{SD}+1)}{(b_M)^{t_{SD}+1}} C_{t_{SD}+1+(t_{RD}+1)(R-|\bar{\Psi}_j|)}\\ &\times \prod_{r=|\bar{\Psi}_j|+1}^{R} \left\{\frac{a_{RD}^{(r)}\Gamma(t_{RD}+1)}{(b_M)^{t_{RD}+1}}\right\} \prod_{r=1}^{|\bar{\Psi}_j|} \left\{\frac{a_{SR}^{(r)}\Gamma(t_{SR}+1)}{(b_M)^{t_{SR}+1}} C_{t_{SR}+1}\right\}\\ &\times \left(\frac{\eta_0}{P}\right)^{t_{SD}+R+1+Rt_{RD}+|\bar{\Psi}_j|(t_{SR}-t_{RD})},\end{aligned} \tag{41}$$

which is a geometric program that can be readily solved using convex solvers such as CVX [23]. The next sections demonstrate the applications of the framework developed above for multiple-relay cooperative systems in various practical scenarios.

IV. Applications

One of the important aspects of the proposed framework is that the results provided above are applicable in many scenarios for fading distributions and PHY layer transmission schemes such as space-time coding, cooperative beamforming or antenna selection etc. These schemes or a combination of these can be therefore adopted by the nodes of the cooperative $\mathcal{P}_0, \mathcal{P}_m$ systems to further enhance reliability and performance of communication. The analyses pertaining to such systems are developed below. It can also be noted that due to page limitations, the analysis of other practically relevant systems is given in detail in the technical report [25].

A. MIMO-OSTBC Based Multi-Relay Cooperative Systems

OSTBCs are ideally suited for attaining beneficial diversity gains in multiple-input multiple-output (MIMO) systems since they achieve the full diversity gain despite using low-complexity linear processing at the receiver. Furthermore, they do not require any feedback of the channel state information from the receiver, thus resulting in no overheads. Thus, MIMO-OSTBC schemes have been the focus of [16], [26]. The proposed framework can be readily extended to the analysis of such cooperative MIMO-OSTBC systems, as demonstrated in this section. Let us consider a multi-relay aided cooperative scenario relying on multiple antenna assisted source and relay nodes, each with $N_s = N_r = N$ antennas, since the source and relays employ the same complex OSTBC design of either a square or non-square matrix. Let N_d denote the number of antennas at the destination node. This standard cooperative OSTBC system model is similar to the ones considered in [27]. Due to OSTBC based transmission, this scheme does not require CSI at the transmitter, whereas for decoding purposes it is assumed that perfect channel knowledge is available at each of the receiving nodes. The received codewords $\mathbf{Y}_{SD} \in \mathbb{C}^{N_d \times T}, \mathbf{Y}_{SR}^{(r)} \in \mathbb{C}^{N \times T}$ at the destination and relay r respectively in the first phase corresponding to the broadcast from the source with power P_0 are given as

$$\begin{aligned}\mathbf{Y}_{SD} =& \sqrt{\frac{P_0}{NR_c}}\mathbf{H}_{SD}\mathbf{X} + \mathbf{W}_{SD},\\ \mathbf{Y}_{SR}^{(r)} =& \sqrt{\frac{P_0}{NR_c}}\mathbf{H}_{SR}^{(r)}\mathbf{X} + \mathbf{W}_{SR}^{(r)},\end{aligned} \tag{42}$$

where T is the block length, R_c denotes the OSTBC rate and $\mathbf{X} \in \mathbb{C}^{N \times T}$ represents the OSTBC transmit matrix. The matrices $\mathbf{H}_{SD}$ and $\mathbf{H}_{SR}^{(r)}$ are the MIMO channel matrices between the source and destination, source and relay r, respectively. The codeword $\mathbf{Y}_{RD}^{(r)} \in \mathbb{C}^{N_d \times T}$ received at the destination during the subsequent relay transmission phase is expressed as

$$\mathbf{Y}_{RD}^{(r)} = \sqrt{\frac{P_r}{NR_c}}\mathbf{H}_{RD}^{(r)}\mathbf{X} + \mathbf{W}_{RD}^{(r)}, \tag{43}$$

where P_r is the power at relay r and $\mathbf{H}_{RD}^{(r)}$ denotes the MIMO channel matrix between relay r and the destination node. The instantaneous SNRs of the source-destination, source-relay r, and relay r-destination links can be seen to be given as,

$\gamma_{SD} = \frac{P_0||\mathbf{H}_{SD}||_F^2}{R_c N \eta_0} = \beta_{SD}\bar{\gamma}_{SD}$ [28], $\gamma_{SR}^{(r)} = \frac{P_0\left|\left|\mathbf{H}_{SR}^{(r)}\right|\right|_F^2}{R_c N \eta_0} = \beta_{SR}^{(r)}\bar{\gamma}_{SR}^{(r)}$, and $\gamma_{RD}^{(r)} = \frac{P_r\left|\left|\mathbf{H}_{RD}^{(r)}\right|\right|_F^2}{R_c N \eta_0} = \beta_{RD}^{(r)}\bar{\gamma}_{RD}^{(r)}$ respectively, where $\beta_{SD}, \beta_{SR}^{(r)}$ and $\beta_{RD}^{(r)}$ are defined as $\beta_{SD} = \frac{||\mathbf{H}_{SD}||_F^2}{NR_c}$, $\beta_{SR}^{(r)} = \frac{\left|\left|\mathbf{H}_{SR}^{(r)}\right|\right|_F^2}{NR_c}$, $\beta_{RD}^{(r)} = \frac{\left|\left|\mathbf{H}_{RD}^{(r)}\right|\right|_F^2}{NR_c}$. To illustrate the applicability of the results derived, consider the coefficients of the channel matrices $\mathbf{H}_{SD}, \mathbf{H}_{SR}^{(r)}$ and $\mathbf{H}_{RD}^{(r)}$ to be the Nakagami-m fading with parameters (m_{SD}, δ_{SD}^2), $\left(m_{SR}^{(r)}, \left(\delta_{SR}^{(r)}\right)^2\right)$, and $\left(m_{RD}^{(r)}, \left(\delta_{RD}^{(r)}\right)^2\right)$, respectively. Therefore, β_{SD} is Gamma distributed with the PDF of:

$$f_{\beta_{SD}}(x) = \left(\frac{NR_c m_{SD}}{\delta_{SD}^2}\right)^{NN_d m_{SD}} \frac{x^{NN_d m_{SD}-1}}{(NN_d m_{SD}-1)!} \times \exp\left(-\frac{R_c N m_{SD} x}{\delta_{SD}^2}\right). \quad (44)$$

Using the identity $\exp(-x) = \sum_{j=0}^{\infty}(-x)^j/j!$, the above expression for $f_{\beta_{SD}}(x)$ can be rewritten as

$$\begin{aligned} f_{\beta_{SD}}(x) = &\left(\frac{NR_c m_{SD}}{\delta_{SD}^2}\right)^{NN_d m_{SD}} \frac{x^{NN_d m_{SD}-1}}{(NN_d m_{SD}-1)!} \\ &\times \sum_{j=0}^{\infty} \frac{1}{j!}\left(-\frac{R_c N m_{SD} x}{\delta_{SD}^2}\right)^j \\ =&a_{SD} x^{t_{SD}} + o(x^{t_{SD}+\epsilon}). \end{aligned} \quad (45)$$

Considering the term corresponding to the summation index $j = 0$ in the above expression, the parameters a_{SD} and t_{SD} for the source-destination link can be obtained as

$$\begin{aligned} a_{SD} =& \frac{1}{(NN_d m_{SD}-1)!}\left(\frac{NR_c m_{SD}}{\delta_{SD}^2}\right)^{NN_d m_{SD}}, \\ t_{SD} =& NN_d m_{SD} - 1. \end{aligned}$$

Similarly, one can determine the respective parameter values for the SR and RD channels as

$$\begin{aligned} a_{SR}^{(r)} =& \frac{1}{\left(N^2 m_{SR}^{(r)} - 1\right)!}\left(\frac{NR_c m_{SR}^{(r)}}{\left(\delta_{SR}^{(r)}\right)^2}\right)^{N^2 m_{SR}^{(r)}}, \\ t_{SR}^{(r)} =& N^2 m_{SR}^{(r)} - 1, \\ a_{RD}^{(r)} =& \frac{1}{\left(NN_d m_{RD}^{(r)} - 1\right)!}\left(\frac{NR_c m_{RD}^{(r)}}{\left(\delta_{RD}^{(r)}\right)^2}\right)^{NN_d m_{RD}^{(r)}}, \\ t_{RD}^{(r)} =& NN_d m_{RD}^{(r)} - 1. \end{aligned}$$

The parameter values above can now be substituted into the results derived in Section II-B, specifically into (4) for the end-to-end SER and into (12) for the optimal power sharing, to obtain the desired results for the dual-phase MIMO-OSTBC multi-relay system over Nakagami-m fading channels. One can also derive the corresponding results for the multi-phase MIMO-OSTBC multi-relay system communicating over Nakagami-m fading links, using the same parameters above, together with $a_{RR}^{(q,r)} = \frac{1}{\left(N^2 m_{RR}^{(q,r)}-1\right)!}\left(\frac{NR_c m_{RR}^{(q,r)}}{\left(\delta_{RR}^{(q,r)}\right)^2}\right)^{N^2 m_{RR}^{(q,r)}}$, $t_{RR}^{(q,r)} = N^2 m_{RR}^{(q,r)} - 1$ in the results for end-to-end SER and optimal power allocation derived in (25) and (29) respectively in Section III. Furthermore, using these parameter values, it can be readily seen that the diversity orders of the $\mathcal{P}_0, \mathcal{P}_m$ based MIMO-OSTBC cooperative schemes communicating over Nakagami-m fading links with $m_{SR}^{(r)} = m_{SR}, m_{RD}^{(r)} = m_{RD}, \forall r$ are

$$\begin{aligned} d_{\text{OSTBC}} =& t_{SD} + 1 + R(\min\{t_{SR}, t_{RD}\} + 1) \\ =& NN_d m_{SD} + RN \min\{m_{SR}N, m_{RD}N_d\}. \end{aligned} \quad (46)$$

The above results illustrate that the diversity order of the cooperative MIMO system depends not only on the number of relays and antennas at the source, relay, and destination nodes, but also on the fading parameters of the various links.

B. Multi-Relay SISO Cooperative Systems with Cooperative Beamforming

Cooperative beamforming can be achieved by the relays to form a 'virtual' antenna array, thus gleaming advantages similar to those of multi-antenna systems with the aid of single antenna relays. Careful selection of the beamforming weights in such a system can lead to a significant improvement of the diversity order and in turn of the reliability of signal reception at the destination node. Furthermore, this technique has been shown to be ideally suited for cognitive radio networks [29], [30] as well as for physical layer security [31]. The results derived for this system employing the proposed framework are described below. Consider a cooperative beamforming-based multi-relay SISO cooperative $\mathcal{P}_0$ system in which the set of relays Ψ_j that decode the signal correctly transmit in the second phase simultaneously in the same band. Note that since orthogonal channels are not required by the multiple relays, this results in significant savings in terms of bandwidth. The signal received at the destination and relay r in phase I can be modeled as

$$y_{SD} = \sqrt{P_0} h_{SD} x + w_{SD}, \quad y_{SR}^{(r)} = \sqrt{P_0} h_{SR}^{(r)} x + w_{SR}^{(r)}, \quad (47)$$

where x denotes the M-PSK or M-QAM modulated symbol, w_{SD}, $w_{SR}^{(r)}$ are the additive white Gaussian noise (AWGN) noise terms with variance $\eta_0/2$ and h_{SD}, $h_{SR}^{(r)}$ are the fading channel coefficients between the source and destination, source and r^{th} relay, respectively. Using the above equations, the instantaneous SNRs at the destination and relay nodes can be derived as, $\gamma_{SD} = \frac{P_0|h_{SD}|^2}{\eta_0} = \beta_{SD}\bar{\gamma}_{SD}$ and $\gamma_{SR}^{(r)} = \frac{P_0\left|h_{SR}^{(r)}\right|^2}{\eta_0} = \beta_{SR}^{(r)}\bar{\gamma}_{SR}^{(r)}$, where the parameters β_{SD} and $\beta_{SR}^{(r)}$ are defined as $\beta_{SD} = |h_{SD}|^2$ and $\beta_{SR}^{(r)} = \left|h_{SR}^{(r)}\right|^2$. In the subsequent relaying phase, the relays in the set Ψ_j simultaneously retransmit the symbol x to the destination using the beamforming coefficients $\{\mathcal{B}_r, \forall r \in \Psi_j\}$. The aggregate signal received at the destination can be expressed as

$$y_{RD} = \sum_{r\in\Psi_j} \sqrt{P_r}\mathcal{B}_r h_{RD}^{(r)} x + w_{RD}, \quad (48)$$

where w_{RD} is the symmetric complex AWGN at the destination with a variance of $\eta_0/2$ per dimension and $h_{RD}^{(r)}$ is the fading channel coefficient between relay r and the destination. Using the optimal maximal ratio combining beamforming coefficients $\mathcal{B}_r = \sqrt{\frac{1}{\sum_{r'\in\Psi_j}\left|h_{RD}^{(r')}\right|^2}}\left(h_{RD}^{(r)}\right)^*$ for all $r \in \Psi_j$ [12], the instantaneous SNR at the destination can be expressed as, $\gamma_{RD} = \sum_{r\in\Psi_j} \frac{P_r\left|h_{RD}^{(r)}\right|^2}{\eta_0} = \sum_{r\in\Psi_j} \beta_{RD}^{(r)}\bar{\gamma}_{RD}^{(r)}$, where $\beta_{RD}^{(r)} = \left|h_{RD}^{(r)}\right|^2$. Therefore, substituting the parameters (a_{SD}, t_{SD}), $\left(a_{SR}^{(r)}, t_{SR}^{(r)}\right)$, and $\left(a_{RD}^{(r)}, t_{RD}^{(r)}\right)$ for the PDFs of $\beta_{SD}, \beta_{SR}^{(r)}$, and $\beta_{RD}^{(r)}$ from Table II into the expression for Pr(e) in (4), one can readily obtain the end-to-end probability of error for cooperative beamforming in various fading scenarios. These parameters can be further substituted into (12) in Section II-B to obtain the optimal power fractions at the source and relays.

C. FSO Based Multi-Relay Cooperative Systems

Free space optical (FSO) relaying systems have recently gained significant popularity due to their low cost and rapid deployability [32]. Furthermore, FSO systems have the ability to support higher data-rates and use license-free spectrum for operation, thus making them ideally suited for communication applications. Extension of the cooperative communication paradigm to FSO systems has been proposed by Anees and Bhatnagar [33], [34]. These systems employ the subcarrier intensity modulation (SIM) technique for transmission of M-ary PSK modulated optical symbols over FSO links, as described in [35]. In such a system, the signals received at the r^{th} relay and destination nodes after optical-to-electrical conversion are given as

$$\begin{aligned} y_{SD} =& \eta_{SD}\sqrt{P_0} I_{SD} x + w_{SD}, \\ y_{SR}^{(r)} =& \eta_{SR}^{(r)}\sqrt{P_0} I_{SR}^{(r)} x + w_{SR}^{(r)}, \end{aligned} \tag{49}$$

where η_{SD} and $\eta_{SR}^{(r)}$ are the optical-to-electrical conversion coefficients, x denotes the transmitted symbol, while I_{SD} and $I_{SR}^{(r)}$ represent the real-valued irradiances of the SD and SR links with $\mathbb{E}\{I_{SD}\} = 1$, $\mathbb{E}\left\{I_{SR}^{(r)}\right\} = 1$. The quantities w_{SD} and $w_{SR}^{(r)}$ are the complex-valued AWGN samples with a mean of 0 and a variance of $\eta_0/2$ per dimension. It is assumed that each relay has channel knowledge for its respective SR link, whereas the destination node has channel knowledge of the SD and all the RD links for coherent detection. The instantaneous SNRs at each relay r and destination node in the first phase can be expressed as $\gamma_{SR}^{(r)} = \beta_{SR}^{(r)}\bar{\gamma}_{SR}^{(r)}$, $\gamma_{SD} = \beta_{SD}\bar{\gamma}_{SD}$ where $\beta_{SR}^{(r)} = \left(\eta_{SR}^{(r)}\right)^2\left(I_{SR}^{(r)}\right)^2$ and $\beta_{SD} = \eta_{SD}^2 I_{SD}^2$. Similarly, one can express the instantaneous SNR at the destination node in the second phase as, $\gamma_{RD}^{(r)} = \beta_{RD}^{(r)}\bar{\gamma}_{RD}^{(r)}$, where $\beta_{RD}^{(r)} = \left(\eta_{RD}^{(r)}\right)^2\left(I_{RD}^{(r)}\right)^2$. Let us consider now the FSO links to be Gamma-Gamma distributed with shape parameters of (μ_{SD}, ν_{SD}), $\left(\mu_{SR}^{(r)}, \nu_{SR}^{(r)}\right)$, and $\left(\mu_{RD}^{(r)}, \nu_{RD}^{(r)}\right)$ corresponding to the source-destination, source-relay r, and relay r-destination links, respectively. The PDF of β_{SD} denoted by $f_{\beta_{SD}}(x)$ can be obtained as [33]

$$\begin{aligned} f_{\beta_{SD}}(x) =& \sum_{k=0}^{\infty}\left(\zeta_k(\nu_{SD}, \mu_{SD}) x^{\frac{\nu_{SD}+k}{2}-1}\right) \\ &+ \sum_{k=0}^{\infty}\left(\zeta_k(\mu_{SD}, \nu_{SD}) x^{\frac{\mu_{SD}+k}{2}-1}\right), \end{aligned} \tag{50}$$

where $\zeta_k(a, b)$ is defined as, $\zeta_k(a, b) = \frac{\pi(ab)^{a+k}}{2(\eta_{SD})^{a+k}\sin((b-a)\pi)k!\Gamma(a)\Gamma(b)\Gamma(a-b+k+1)}$. The parameters (a_{SD}, t_{SD}) corresponding to the PDF above can be obtained by considering the dominant term with $k = 0$ as

$$\begin{aligned} a_{SD} =& \begin{cases} \zeta_0(\nu_{SD}, \mu_{SD}) & \text{if } \nu_{SD} < \mu_{SD} \\ \zeta_0(\mu_{SD}, \nu_{SD}) & \text{if } \nu_{SD} > \mu_{SD}, \end{cases} \\ t_{SD} =& \min\{\nu_{SD}, \mu_{SD}\}/2 - 1. \end{aligned}$$

Similarly, one can derive these parameters for the source-relay r, relay r-relay q, and relay r-destination links as

$$\begin{aligned} a_{SR}^{(r)} =& \begin{cases} \zeta_0\left(\nu_{SR}^{(r)}, \mu_{SR}^{(r)}\right) & \text{if } \nu_{SR}^{(r)} < \mu_{SR}^{(r)} \\ \zeta_0\left(\mu_{SR}^{(r)}, \nu_{SR}^{(r)}\right) & \text{if } \nu_{SR}^{(r)} > \mu_{SR}^{(r)} \end{cases} \\ t_{SR}^{(r)} =& \min\{\nu_{SR}^{(r)}, \mu_{SR}^{(r)}\}/2 - 1, \\ a_{RR}^{(q,r)} =& \begin{cases} \zeta_0\left(\nu_{RR}^{(q,r)}, \mu_{RR}^{(q,r)}\right) & \text{if } \nu_{RR}^{(q,r)} < \mu_{RR}^{(q,r)} \\ \zeta_0\left(\mu_{RR}^{(q,r)}, \nu_{RR}^{(q,r)}\right) & \text{if } \nu_{RR}^{(q,r)} > \mu_{RR}^{(q,r)} \end{cases} \\ t_{RR}^{(q,r)} =& \min\{\nu_{RR}^{(q,r)}, \mu_{RR}^{(q,r)}\}/2 - 1, \end{aligned}$$

$$\begin{aligned} a_{RD}^{(r)} =& \begin{cases} \zeta_0\left(\nu_{RD}^{(r)}, \mu_{RD}^{(r)}\right) & \text{if } \nu_{RD}^{(r)} < \mu_{RD}^{(r)} \\ \zeta_0\left(\mu_{RD}^{(r)}, \nu_{RD}^{(r)}\right) & \text{if } \nu_{RD}^{(r)} > \mu_{RD}^{(r)} \end{cases} \\ t_{RD}^{(r)} =& \min\{\nu_{RD}^{(r)}, \mu_{RD}^{(r)}\}/2 - 1. \end{aligned}$$

Thus, substituting the above parameters into (24) and (39) respectively, one can now derive the diversity orders of the $\mathcal{P}_0$ and $\mathcal{P}_m$ based multi-relay systems communicating over Gamma-Gamma distributed FSO links with $t_{SR}^{(r)} = t_{SR}$ and $t_{RD}^{(r)} = t_{RD}, \forall r$ as

$$\begin{aligned} d_{\text{FSO}} =& t_{SD} + 1 + R(\min\{t_{SR}, t_{RD}\} + 1) \\ =& \frac{1}{2}\Big[\min\{\nu_{SD}, \mu_{SD}\} \\ &+ R\min\Big\{\min\left\{\nu_{SR}^{(r)}, \mu_{SR}^{(r)}\right\}, \min\left\{\nu_{RD}^{(r)}, \mu_{RD}^{(r)}\right\}\Big\}\Big]. \end{aligned} \tag{51}$$

Furthermore, these parameters can also be substituted into (12) and (29) to obtain the optimal power fractions.

D. Transmit and Receive Antenna Selection Based Multi-Relay Cooperative Systems

It is widely recognized that multiple antennas at the transmitter and receiver significantly improve the reliability of communication through diversity. However, this also leads to an increased signal processing complexity as well as to increased higher device costs due to the individual RF chains required for signal reception at the multiple antennas. Intelligent antenna selection can enhance the practical appeal of such systems by reducing their complexity and cost, while retaining their diversity advantages [36], [37]. The proposed framework can be exploited for the analysis of cooperative systems with antenna selection at the source, destination and individual relay nodes, as demonstrated below.

Consider a $\mathcal{P}_0$ and $\mathcal{P}_m$ based selective DF wireless cooperative system using N_s, N_r, and N_d antennas at the source, relay and destination nodes, respectively. The transmit and receive antenna selection is based on instantaneous SNR maximization at the destination node, as per the procedure detailed below. In the first step, the i^{th} transmit antenna at the source and n^{th} receive antenna at the destination are selected for ensuring the direct SD SISO link has the maximum channel gain amongst all the N_dN_s SD links. In the second step, a single receive antenna is selected at each relay based on the maximum channel gain from amongst the N_r channels emanating from the i^{th} antenna at the source to each relay. This is denoted by k_r, where the subscript r represents relay r. In the final step, the $(\tilde{k}_r)^{\text{th}}$ antenna at relay r and $(\tilde{n}_r)^{\text{th}}$ antenna at the destination node are selected based on the maximum channel gain of all the N_dN_r links between relay r and the destination nodes. The instantaneous SNR at the destination in the first phase is

$$\begin{aligned}\gamma_{SD} =& \max_{i=1,2,.,N_s;n=1,2,.,N_d}\left\{\gamma_{SD_{in}}=\frac{P_0|h_{SD_{in}}|^2}{\eta_0}\right\}\\ =&\beta_{SD}\bar{\gamma}_{SD},\end{aligned} \tag{52}$$

where $\beta_{SD}=\max\limits_{i;n}\left\{|h_{SD_{in}}|^2\right\}=\max\limits_{i;n}\{\beta_{SD_{in}}\}$. For purposes of illustration, assume the source-destination, source-relay r, and relay r-destination links to be Nakagami-m faded with parameters (m_{SD},δ_{SD}^2), $(m_{SR}^{(r)},(\delta_{SR}^{(r)})^2)$, and $(m_{RD}^{(r)},(\delta_{RD}^{(r)})^2)$, respectively. One can now employ the expression for the PDF $f_{\beta_{SD_{in}}}(x)$ of the Gamma distributed random variable $\beta_{SD_{in}}$, to calculate the parameters a_{SD} and t_{SD} as follows. The CDF and PDF of β_{SD} denoted by $F_{\beta_{SD}}(x)$ and $f_{\beta_{SD}}(x)$ respectively, are

$$\begin{aligned}F_{\beta_{SD}}(x)=&Pr\Big(\max_{i=1,\cdots,N_s;n=1,\cdots,N_d}(\beta_{SD_{in}})\leq x\Big)\\ =&\left(F_{\beta_{SD_{in}}}(x)\right)^{N_sN_d},\end{aligned} \tag{53}$$

where $F_{\beta_{SD_{in}}}(x)$ is the CDF of the quantity $\beta_{SD_{in}}$. Differentiating the above equation with respect to x, the PDF $f_{\beta_{SD}}(x)$ can be obtained as

$$\begin{aligned}f_{\beta_{SD}}(x)=&N_sN_d\left(F_{\beta_{SD_{in}}}(x)\right)^{N_sN_d-1}f_{\beta_{SD_{in}}}(x)\\ =&N_sN_d\left(\frac{\gamma\left(m_{SD},m_{SD}x/\delta_{SD}^2\right)}{(m_{SD}-1)!}\right)^{N_sN_d-1}\\ &\times\frac{x^{m_{SD}-1}\exp\left(-m_{SD}x/\delta_{SD}^2\right)}{(\delta_{SD}^2/m_{SD})^{m_{SD}}(m_{SD}-1)!}.\end{aligned} \tag{54}$$

Furthermore, using the identities $\gamma(s,x)=x^s\Gamma(s)\exp(-x)\times\sum_{k=0}^{\infty}\frac{x^k}{\Gamma(s+k+1)}$ from [(8.2.6, 8.7.1), [38]] and $\exp(-x)=\sum_{j=0}^{\infty}(-x)^j/j!$, the above expression can be simplified to yield the values of a_{SD}, t_{SD} as [1]

$$a_{SD}=\frac{N_sN_d(m_{SD}/\delta_{SD}^2)^{m_{SD}N_sN_d}}{(m_{SD})^{N_sN_d-1}((m_{SD}-1)!)^{N_sN_d}},t_{SD}=m_{SD}N_dN_s-1.$$

Similarly, the parameters $\left(a_{RD}^{(r)},t_{RD}^{(r)}\right)$ for the RD links can be obtained using the PDF $f_{\beta_{RD}^{(r)}}(\cdot)$ as

$$a_{RD}^{(r)}=\frac{N_rN_d\left(m_{RD}^{(r)}/\left(\delta_{RD}^{(r)}\right)^2\right)^{m_{RD}^{(r)}N_rN_d}}{\left(m_{RD}^{(r)}\right)^{N_rN_d-1}\left(\left(m_{RD}^{(r)}-1\right)!\right)^{N_rN_d}},t_{RD}^{(r)}=m_{RD}^{(r)}N_dN_r-1.$$

The received SNR at the $(k_r)^{\text{th}}$ antenna of relay r corresponding to transmission by the i^{th} source antenna chosen in the first phase is obtained as

$$\gamma_{SR}^{(r)}=\max_{k_r=1,\cdots,N_r}\left\{\frac{P_0\left|h_{SR_{ik_r}}^{(r)}\right|^2}{\eta_0}\right\}=\beta_{SR}^{(r)}\bar{\gamma}_{SR}^{(r)}, \tag{55}$$

where $\beta_{SR}^{(r)}=\max\limits_{k_r=1,\cdots,N_r}\left\{\left|h_{SR_{ik_r}}^{(r)}\right|^2\right\}=\max\limits_{k_r=1,\cdots,N_r}\left\{\beta_{SR_{ik_r}}^{(r)}\right\}$. Following a procedure similar to the one described above for the SD link, the parameters $a_{SR}^{(r)}, t_{SR}^{(r)}$ are determined as

$$a_{SR}^{(r)}=\frac{N_r\left(m_{SR}^{(r)}/\left(\delta_{SR}^{(r)}\right)^2\right)^{m_{SR}^{(r)}N_r}}{\left(m_{SR}^{(r)}\right)^{N_r-1}\left(\left(m_{SR}^{(r)}-1\right)!\right)^{N_r}},t_{SR}^{(r)}=m_{SR}^{(r)}N_r-1.$$

The above parameters can be employed in the relevant results in Section II-B for the analysis of the $\mathcal{P}_0$ cooperative system with transmit and receive antenna selection. For the $\mathcal{P}_m$ system, consider the antenna selected at each relay in the third step of the procedure described above used for inter-relay communication. The relevant parameters for transmission from relay r to q can be expressed as $a_{RR}^{(q,r)}=\frac{\left(m_{RR}^{(q,r)}/\left(\delta_{RR}^{(q,r)}\right)^2\right)^{m_{RR}^{(q,r)}}}{\left(m_{RR}^{(q,r)}-1\right)!}, t_{RR}^{(q,r)}=m_{RR}^{(q,r)}-1$ using the Nakagami-m fading PDF $f_{\beta_{RR}^{(q,r)}}(\cdot)$. These can in turn be substituted into the results of Section III. Using values of $t_{SR}^{(r)}, t_{SD}$ and $t_{RD}^{(r)}$ above in (24) or (39), the identical diversity order of the $\mathcal{P}_0$ and $\mathcal{P}_m$ systems with transmit and receive antenna selection over Nakagami-m faded links, assuming $t_{SR}^{(r)}=t_{SR}$ and $t_{RD}^{(r)}=t_{RD},\forall r$, is expressed

$$\begin{aligned}d_{\text{TRAS}}=&t_{SD}+1+R(\min\{t_{SR},t_{RD}\}+1)\\ =&m_{SD}N_sN_d+RN_r\min\{m_{SR},m_{RD}N_d\}.\end{aligned} \tag{56}$$

The parameters can also be substituted into (12) and (29) to obtain the optimal power fractions for transmit and receive antenna selection in both two-phase and multi-phase multi-relay aided cooperative systems.

V. Simulation Results

This section presents simulation results for validating the proposed framework and derived results for the multi-relay cooperative systems for the various PHY layer and signal processing schemes considered above. For simulation purposes, consider the transmission of QPSK modulated symbols, i.e. $M=4$ at a noise power of $\eta_0/2=0.5$ per dimension. Fig. 3 plots the SER performance of the dual-phase and multi-phase $\mathcal{P}_m, m=1$ protocol based selective DF SISO cooperative

Fading conditions	$\mathcal{P}_0, \alpha_0$	$\mathcal{P}_0, \alpha_1$	$\mathcal{P}_0, \alpha_2$	$\mathcal{P}_1, \alpha_0$	$\mathcal{P}_1, \alpha_1$	$\mathcal{P}_1, \alpha_2$
$\eta-\mu$ fading links with $\eta=1, \mu=0.5$ [Format 1]	0.6974	0.1513	0.1513	0.6988	0.1069	0.1943
$\kappa-\mu$ fading links with $\kappa=0, \mu=0.5$	0.6669	0.1666	0.1666	0.6635	0.1190	0.2175

TABLE III

OPTIMAL POWER FRACTIONS FOR DIFFERENT FADING CHANNEL CONDITIONS WITH $\delta_{SD}^2 = \delta_{SR}^2 = 0.1$ AND $\delta_{RD}^2 = 1$.

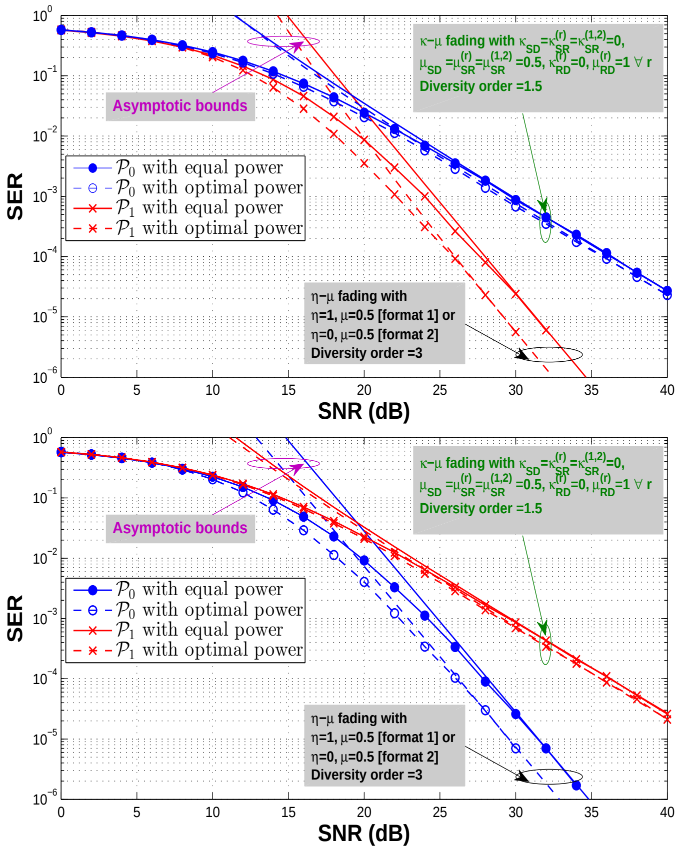

Fig. 3. SER performance of the $\mathcal{P}_0$ and $\mathcal{P}_m, m{=}1$ based selective DF SISO cooperative systems with $R{=}2$ relays, $N_s{=}N_r{=}N_d{=}1$, noise power $\eta_0{=}1$, and $\delta_{SD}^2{=}\delta_{SR}^2{=}0.1, \delta_{RD}^2{=}1$, where analytical expressions (4), (25) with $\eta-\mu$ and $\kappa-\mu$ fading parameters given in Table II are simulated to plot asymptotic bounds, and (12) and (40) are used to obtain optimal power fractions at the source and both the relays.

system over independent and possibly non-identical $\eta-\mu$ and $\kappa-\mu$ distributed SR, RD and SD links. It can be seen from Fig. 3 that the asymptotic SER approximations derived in (4) and (25) for the dual-phase and multi-phase protocols respectively are in close agreement with the simulation results at high SNRs. These plots also validate the expressions derived for the diversity order in Sections II-B1, III-B1 for the dual and multi-phase protocols respectively, and demonstrate that the proposed multi-relay schemes achieve a diversity order of $d = t_{SD} + 1 + R(\min\{t_{SR}, t_{RD}\} + 1) = \mu_{SD} + R\min\{\mu_{SR}, \mu_{RD}\} = 1.5$ and $d = t_{SD} + 1 + R(\min\{t_{SR}, t_{RD}\} + 1) = 2\mu_{SD} + 2R\min\{\mu_{SR}, \mu_{RD}\} = 3$ under $\kappa-\mu$ and $\eta-\mu$ fading conditions respectively, with $t_{SR}^{(r)} = t_{SR}$ and $t_{RD}^{(r)} = t_{RD}$ for $r = 1, 2, \cdots, R$. Furthermore, Fig. 3 also plots the simulated SER performance for both the multi-relay protocols with the optimal source-relay power sharing, obtained using the results in (12) and (40), respectively. It can be clearly seen that the optimal power fractions specified in Table III significantly improve the end-to-end SER of the systems. Furthermore, it can be observed from Table III that when the RD links are relatively strong in comparison to the SR links, more power is allocated to the source in comparison to the relays in both the $\mathcal{P}_0$ as well as $\mathcal{P}_m$ schemes. The remaining power is equally shared amongst both the relays in the $\mathcal{P}_0$ scheme, whereas in the $\mathcal{P}_1$ scheme, the power allocated to the second relay is higher than that allocated to the first relay. This can be expected, since the second relay is more reliable than the first relay in the $\mathcal{P}_1$ scheme, as it combines the signals from both the source and the first relay prior to decoding, while the first relay decodes only the signal received from the source.

Fig. 4 demonstrates the SER performance of $\mathcal{P}_0$ and $\mathcal{P}_m, m = 1$ based multi-relay cooperative systems using QPSK modulated Alamouti coded MIMO-OSTBC transmission. For simulation purposes, the Nakagami fading parameters of each link are set to unity. In Fig. 4, the SER plots are shown for equal power sharing, i.e. for $\alpha_0 = \alpha_1 = \alpha_2 = \frac{1}{3}$ and optimal power sharing for the scenarios when either the RD link is stronger than the SR link or both the links have equal channel gains. These results lend support to the claim that the optimal power sharing lead to a considerable end-to-end error rate reduction. Furthermore, a significant SER improvement can be seen for the scenarios when $\frac{\delta_{rd}^2}{\delta_{sd}^2}$ is higher than $\frac{\delta_{sr}^2}{\delta_{sd}^2}$. This arises since a substantial fraction of the power is allocated to the source in comparison to the relays, which translates into a lower probability of error at the relay as well as destination nodes compared to equal power sharing. Furthermore, for the scenarios when the SR link is stronger than the RD links, equal power sharing is optimal for both the multi-relay systems. It can also be seen from Fig. 4 that the MIMO-OSTBC based $\mathcal{P}_0$ and $\mathcal{P}_m, m = 1$ multi-relay cooperative systems achieve a diversity order of $t_{SD} + 1 + R(\min\{t_{SR}, t_{RD}\} + 1) = NN_d m_{SD} + RN\min\{m_{SR}N, m_{RD}N_d\} = 12$.

Fig. 5 portrays the SER performance of the MIMO-ZF based $\mathcal{P}_0$ and $\mathcal{P}_m, m = 1$ multi-relay cooperative systems using $N = 2, N_d = 3$ and all the links experience independent Rayleigh fading with equal channel gains. The net diversity achieved in this scenario is $t_{SD}+1+R(\min\{t_{SR}, t_{RD}\}+1) = 4$, where $t_{SD} = N_d - N = 1, t_{SR} = 0$ and $t_{RD} = N_d - N = 1$, as demonstrated in [25, Section I-A]. It is also interesting to note that the optimal power sharing for the MIMO-OSTBC scenario is independent of the SNR, which arises due to having an equal number of antennas at the source, relay and destination nodes. However, for the MIMO-ZF selective DF cooperative system, where the number of antennas at the des-

SNR (dB)	$\mathcal{P}_0, \alpha_0$	$\mathcal{P}_0, \alpha_1$	$\mathcal{P}_0, \alpha_2$	$\mathcal{P}_1, \alpha_0$	$\mathcal{P}_1, \alpha_1$	$\mathcal{P}_1, \alpha_2$
0	0.3512	0.3244	0.3244	0.3431	0.3218	0.3351
5	0.3793	0.3103	0.3103	0.3620	0.3025	0.3356
10	0.4321	0.2459	0.2459	0.4079	0.2649	0.3272

TABLE IV
OPTIMAL POWER FRACTIONS FOR MIMO-ZF BASED $\mathcal{P}_0$ AND $\mathcal{P}_1$ MULTI-RELAY COOPERATIVE SYSTEMS WITH $N = 2, N_d = 3$.

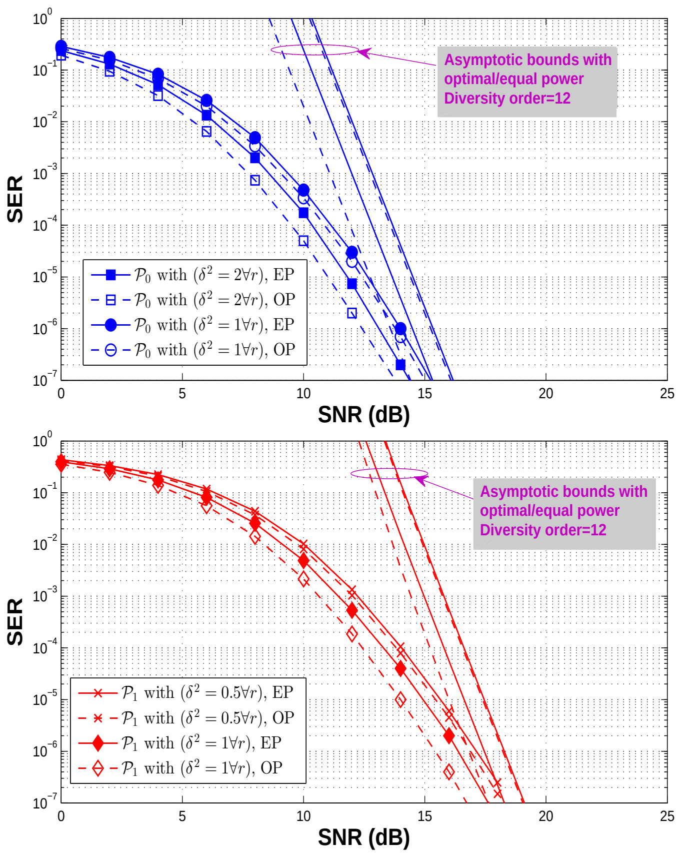

Fig. 4. SER performance of the $\mathcal{P}_0$ and $\mathcal{P}_m, m$=1 based selective DF MIMO-OSTBC cooperative systems with R=2 relays, N_s=N_r=N_d=2, and noise power $\eta_0 = 1$, where analytical expressions (4), (25) with the parameters obtained in Section IV-A are simulated to plot asymptotic bounds, and (12) and (40) are used to obtain optimal power fractions at the source and both the relays.

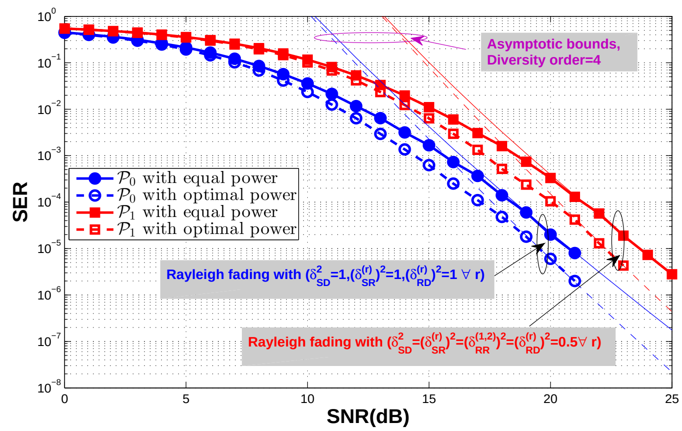

Fig. 5. SER performance of $\mathcal{P}_0$ and $\mathcal{P}_m, m = 1$ based selective DF MIMO-ZF cooperative systems with $R = 2$ relays, $N_s = N_r = 2, N_d = 3$, and noise power $\eta_0 = 1$, where analytical expressions (4), (25) with the parameters obtained in [25, Section I-A] are simulated to plot asymptotic bounds, and (12) and (40) are used to obtain optimal power fractions at the source and both the relays.

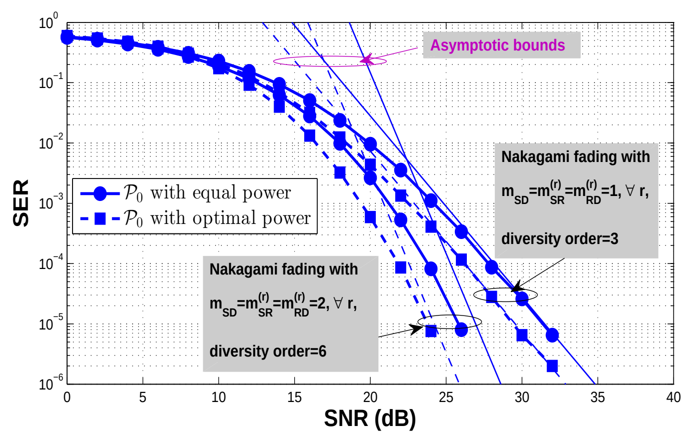

Fig. 6. SER performance of cooperative beamforming in dual-phase $\mathcal{P}_0$ based selective DF cooperative system with $R = 2$ relays, $N_s = N_r = N_d = 2$, and noise power $\eta_0 = 1$, where analytical expression (4) with the parameters obtained in Section IV-B is simulated to plot asymptotic bound, and (12) is used to obtain optimal power fractions at the source and both the relays.

tination is higher than that of the source and relay, the optimal power fraction P_0/P at the source progressively increases with the SNR, as clearly seen in Table IV. This arises, since the diversity orders of the RD links are higher than that of the SR links. Fig. 6 depicts the end-to-end SER performance of our cooperative beamforming based multi-relay systems. For simulation purposes, Nakagami-m fading is considered with average channel gains of $\delta_{SD}^2 = 0.1, \left(\delta_{SR}^{(r)}\right)^2 = 0.1$ and $\left(\delta_{RD}^{(r)}\right)^2 = 1$ for the cooperative beamforming based dual-phase $\mathcal{P}_0$ system. For this system, the diversity order achieved can be readily derived as, $t_{SD}+1+R(\min\{t_{SR}, t_{RD}\}+1) = m_{SD}+R\min\{m_{SR}, m_{RD}\} = 3$ for $m_{SD} = m_{SR}^{(r)} = m_{RD}^{(r)} = 1, \forall r$ and 6 for $m_{SD} = m_{SR}^{(r)} = m_{RD}^{(r)} = 2, \forall r$, which is seen in Fig. 6. Moreover, as shown in Fig. 6, the optimal power fractions derived using (12) can significantly enhance the performance of $\mathcal{P}_0$ based cooperative systems.

Fig. 7 characterizes the performance of $\mathcal{P}_0$ and $\mathcal{P}_m, m = 1$ based cooperative DF FSO systems over Gamma-Gamma distributed links with shape parameters of $\nu_{SD} = \nu_{SR}^{(r)} = \nu_{RD}^{(r)} = \nu_{RR}^{(1,2)} = \nu, \forall r$ and $\mu_{SD} = \mu_{SR}^{(r)} = \mu_{RD}^{(r)} =$

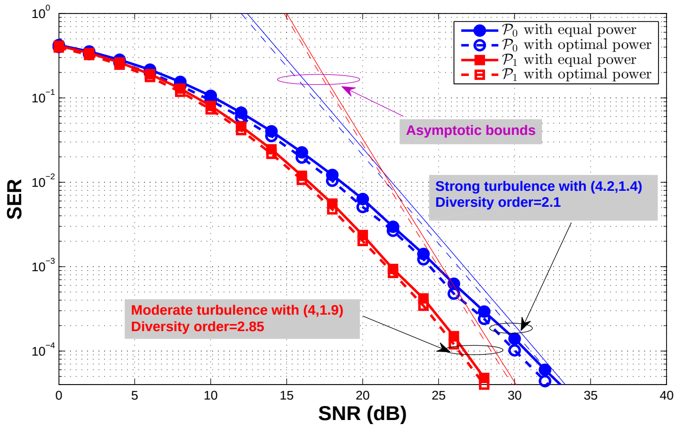

Fig. 7. SER performance of dual-phase $\mathcal{P}_0$ and multi-phase $\mathcal{P}_m, m = 1$ based selective DF FSO cooperative systems with $R = 2$ relays, $N_s = N_r = N_d = 1$, and noise power $\eta_0 = 1$, where analytical expressions (4), (25) with the parameters obtained in Section IV-C are simulated to plot asymptotic bounds, and (12) and (40) are used to obtain optimal power fractions at the source and both the relays.

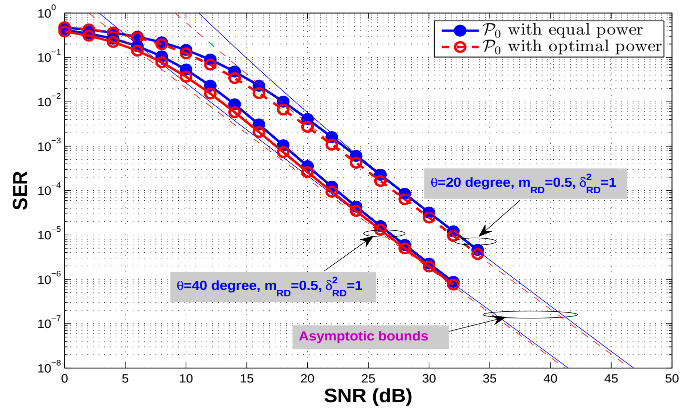

Fig. 8. SER performance of a hybrid satellite-terrestrial system employing dual-phase $\mathcal{P}_0$ protocol with $R = 2$ relays, $N_s = N_r = N_d = 1$, and noise power $\eta_0 = 1$, where analytical expression (4) with the parameters obtained in [25, Section I-C] are simulated to plot asymptotic bound, and (12) is used to obtain optimal power fractions at the source and both the relays.

$\mu_{RR}^{(1,2)} = \mu, \forall r$. In our simulations, QPSK modulated symbols are considered, with optical-to-electrical conversion coefficients of $\eta_{SD} = \eta_{SR}^{(r)} = \eta_{RD}^{(r)} = 1, \forall r$ and $(\mu = 4, \nu = 1.9)$, $(\mu = 4.2, \nu = 1.4)$ for the moderate and strong turbulence regimes, respectively. It can be observed from Fig. 7 that the diversity order achieved for the $\mathcal{P}_0$ and $\mathcal{P}_1$ based multi-relay FSO system is $\frac{1}{2}\Big[\min\{\nu_{SD}, \mu_{SD}\} + R\min\Big\{\min\Big\{\nu_{SR}^{(r)}, \mu_{SR}^{(r)}\Big\}, \min\Big\{\nu_{RD}^{(r)}, \mu_{RD}^{(r)}\Big\}\Big\}\Big] = 2.1$ for the strong turbulence regime and 2.85 for the moderate turbulence regime, respectively. Finally, Fig. 8 presents the SER performance of a $\mathcal{P}_0$ based practical shadowed-Rician land mobile satellite (LMS) system. The detailed analysis of these scenarios is given in the technical report [25] due to lack of space in this paper. It has been shown in [39] that the parameters of a shadowed-Rician LMS channel for the source-relay r and SD links depend on the elevation angle θ as follows, $b(\theta) = -4.7943 \times 10^{-8} \times \theta^3 + 5.5784 \times 10^{-6} \times \theta^2 - 2.1344 \times 10^{-4} \times \theta + 3.2710 \times 10^{-2}$, $m(\theta) = 6.3739 \times 10^{-5} \times \theta^3 + 5.8533 \times 10^{-4} \times \theta^2 - 1.5973 \times 10^{-1} \times \theta + 3.5156$ and $\Omega(\theta) = 1.4428 \times 10^{-5} \times \theta^3 - 2.3798 \times 10^{-3} \times \theta^2 + 1.2702 \times 10^{-1} \times \theta - 1.4864$. For simulation purposes, the elevation angles are set as $\theta_{SD} = \theta_{SR}^{(1)} = \theta_{SR}^{(2)} \in \{20°, 40°\}$ and it is assumed that the channel between relay r and the destination experiences Nakagami-m fading with a parameter of $m_{RD} = 0.5$ and average gain of $\delta_{RD}^2 = 1$. It can be clearly seen from Fig. 8 that the asymptotic SER approximation derived in (4) coincides with the simulation results and also that the system achieves the diversity order of $d_{\text{Hybrid Satellite-Terrestrial}} = 1 + R\min\{1, m_{RD}\} = 2$, as derived in the report [25]. One can also observe that the performance of the hybrid satellite-terrestrial system improves using the optimal power fractions in (12). Furthermore, the end-to-end performance of the system can be significantly enhanced by increasing the elevation angle.

VI. Conclusions

A simplified analytical framework has been presented based on a polynomial approximation of the fading channel PDF to characterize the high-SNR performance of dual-phase $\mathcal{P}_0$ and multi-phase $\mathcal{P}_m$ multi-relay selective DF cooperative communication systems for several fading distributions. The applicability of the proposed framework has been demonstrated through an analysis of the end-to-end SER performance of cooperative systems considering different PHY layer transceiver processing schemes, such as MIMO-OSTBC, MIMO-ZF, cooperative beamforming, transmit antenna selection, amongst others. Furthermore, a framework has also been developed for optimal source-relay power sharing for enhancing the end-to-end performance along with closed-form expressions of the diversity order achieved through cooperative communication. Our simulation results demonstrate the validity of the derived analytical results derived and characterize the performance of diverse cooperative communication systems.

Appendix A
Proof of Theorem 1

For the cooperative system in state ξ_j, since only the relays $r \in \Psi_j$ would selectively retransmit the decoded symbol, the net instantaneous SNR at the destination is

$$\beta_{SD}\bar{\gamma}_{SD} + \sum_{r \in \Psi_j} \beta_{RD}^{(r)}\bar{\gamma}_{RD}^{(r)}. \tag{57}$$

Therefore, the end-to-end conditional symbol error probability for M-ary PSK modulation when the cooperative system is in state ξ_j can be written as [6]

$$\Pr(e|\xi_j, \underline{\beta}) = \frac{1}{\pi}\int_0^{\frac{(M-1)\pi}{M}} \exp\left(-\frac{b_M}{\sin^2\theta}\left(\beta_{SD}\bar{\gamma}_{SD} + \sum_{r \in \Psi_j} \beta_{RD}^{(r)}\bar{\gamma}_{RD}^{(r)}\right)\right) d\theta, \tag{58}$$

where $b_M = \sin^2(\pi/M)$. Averaging over the CSI $\underline{\beta}$, the average probability of symbol error in the state ξ_j can be derived at high SNRs, as shown in Appendix B, as

$$\mathbb{E}_{\underline{\beta}}\{\Pr(e|\xi_j,\underline{\beta})\} \doteq \frac{a_{SD}\Gamma(t_{SD}+1)}{(b_M\bar{\gamma}_{SD})^{t_{SD}+1}} \prod_{r\in\Psi_j} \left\{ \frac{a_{RD}^{(r)}\Gamma\left(t_{RD}^{(r)}+1\right)}{\left(b_M\bar{\gamma}_{RD}^{(r)}\right)^{t_{RD}^{(r)}+1}} \right\} \times C_{t_{SD}+1+\sum_{r\in\Psi_j} t_{RD}^{(r)}+|\Psi_j|}. \quad (59)$$

The quantity $\Pr(\xi_j)$, which denotes the average probability of the system being in state ξ_j, can be expressed as

$$\mathbb{E}_{\underline{\beta}}\{\Pr(\xi_j|\underline{\beta})\} = \prod_{r=1}^{R} \mathbb{E}_{\underline{\beta}}\{\Pr(\xi_j(r)|\underline{\beta})\}, \quad (60)$$

since the links between the source and various relays fade independently. Furthermore, let $e^{(r)}$ denote the event of a decoding error at relay r. Thus, it can be seen that we have:

$$\mathbb{E}_{\underline{\beta}}\{\Pr(\xi_j(r)|\underline{\beta})\} = \begin{cases} \mathbb{E}_{\underline{\beta}}\{P_{S\to R^{(r)}}(e^{(r)}|\underline{\beta})\} & \text{if } \xi_j(r)=0, \\ 1-\mathbb{E}_{\underline{\beta}}\{P_{S\to R^{(r)}}(e^{(r)}|\underline{\beta})\} & \text{if } \xi_j(r)=1. \end{cases} \quad (61)$$

The quantity $\mathbb{E}_{\underline{\beta}}\{P_{S\to R^{(r)}}(e^{(r)}|\underline{\beta})\}$, which denotes the average probability of decoding error at relay r can be evaluated using a procedure similar to the one given in Appendix B for Eq. (59) as

$$\begin{aligned} &\mathbb{E}_{\underline{\beta}}\{P_{S\to R^{(r)}}(e^{(r)}|\underline{\beta})\} \\ &= \frac{1}{\pi}\int_0^{\frac{(M-1)\pi}{M}} \mathbb{E}_{\underline{\beta}}\left\{\exp\left(-\frac{b_M}{\sin^2\theta}\left(\beta_{SR}^{(r)}\bar{\gamma}_{SR}^{(r)}\right)\right)d\theta\right\} \\ &\doteq \frac{a_{SR}^{(r)}\Gamma\left(t_{SR}^{(r)}+1\right)}{\left(b_M\bar{\gamma}_{SR}^{(r)}\right)^{t_{SR}^{(r)}+1}} \times C_{t_{SR}^{(r)}+1}, \end{aligned} \quad (62)$$

where the parameters $\left(a_{SR}^{(r)}, t_{SR}^{(r)}\right)$ depend on the PDF of the source-r^{th} relay fading link. Furthermore, at high SNRs, one can employ the approximation $1-\mathbb{E}_{\underline{\beta}}\{P_{S\to R^{(r)}}(e^{(r)}|\underline{\beta})\} \approx 1$, similar to [6]. This can be seen to yield results that closely approximate the end-to-end performance of our cooperative wireless system. Hence, the expression for $\mathbb{E}_{\underline{\beta}}\{\Pr(\xi_j|\underline{\beta})\}$ given in (60) can be simplified to

$$\begin{aligned} \mathbb{E}_{\underline{\beta}}\{\Pr(\xi_j|\underline{\beta})\} &\doteq \prod_{r\in\bar{\Psi}_j} \mathbb{E}_{\underline{\beta}}\{\Pr(\xi_j(r)|\underline{\beta})\} \\ &= \prod_{r\in\bar{\Psi}_j} \left\{ \frac{a_{SR}^{(r)}\Gamma(t_{SR}^{(r)}+1)}{(b_M\bar{\gamma}_{SR}^{(r)})^{t_{SR}^{(r)}+1}} \times C_{t_{SR}^{(r)}+1} \right\}. \end{aligned} \quad (63)$$

It is worth mentioning that the expressions for $\mathbb{E}_{\underline{\beta}}\{\Pr(e|\xi_j,\underline{\beta})\}$ and $\mathbb{E}_{\underline{\beta}}\{\Pr(\xi_j|\underline{\beta})\}$ considering M-QAM, as shown in Appendix C, are identical to the expressions (59) and (63) derived for M-PSK modulation. However, the quantities b_M and C_n in (59) and (63) for M-QAM are different. Substituting now the expression for $\mathbb{E}_{\underline{\beta}}\{\Pr(\xi_j|\underline{\beta})\}$ from above and that for $\mathbb{E}_{\underline{\beta}}\{\Pr(e|\xi_j,\underline{\beta})\}$ from (59) into (3) yields the expression for the high-SNR end-to-end SER performance of the cooperative wireless system as given in (4), which completes the proof.

Appendix B
Simplification Of $\mathbb{E}_{\underline{\beta}}\{\Pr(e|\xi_j,\underline{\beta})\}$

In order to analyze the behavior of selective DF based cooperative systems at high SNRs, one can now employ the results of Section II-A for the PDFs of the various links at $\beta\to 0^+$ to evaluate the average probability of symbol error, when the cooperative system is in state ξ_j. Exploiting these properties, the average end-to-end SER performance of the dual-phase cooperative wireless system can be simplified as seen in (64). Furthermore, using the identity $\int_0^\infty x^n\exp(-\mu x)dx = \Gamma(n+1)\mu^{-(n+1)}$ [(3.326-2), [22]], it can be seen that

$$\begin{aligned} &\int_0^\infty \exp\left(-\frac{b_M\beta_{SD}\bar{\gamma}_{SD}}{\sin^2\theta}\right) a_{SD}(\beta_{SD})^{t_{SD}} d\beta_{SD} \\ &\qquad = a_{SD}\Gamma(t_{SD}+1)\left(\frac{b_M\bar{\gamma}_{SD}}{\sin^2\theta}\right)^{-(t_{SR}+1)}, \end{aligned} \quad (65)$$

$$\begin{aligned} &\int_0^\infty \exp\left(-\frac{b_M\beta_{RD}^{(r)}\bar{\gamma}_{RD}^{(r)}}{\sin^2\theta}\right) a_{RD}^{(r)}\left(\beta_{RD}^{(r)}\right)^{t_{RD}^{(r)}} d\beta_{RD}^{(r)} \\ &\qquad = a_{RD}^{(r)}\Gamma\left(t_{RD}^{(r)}+1\right)\left(\frac{b_M\bar{\gamma}_{RD}^{(r)}}{\sin^2\theta}\right)^{-\left(t_{RD}^{(r)}+1\right)}, \end{aligned} \quad (66)$$

Hence, using the above integral identities and neglecting the higher-order terms in the polynomial approximation for the PDF at high SNRs, Equation (64) can be simplified to yield the result for $\mathbb{E}_{\underline{\beta}}\{\Pr(e|\xi_j,\underline{\beta})\}$ stated in (59).

Appendix C
Derivations of $\mathbb{E}_{\underline{\beta}}\{\Pr(e|\xi_j,\underline{\beta})\}$ and $\mathbb{E}_{\underline{\beta}}\{\Pr(\xi_j|\underline{\beta})\}$ for M-QAM

The end-to-end conditional symbol error probability for M-ary QAM when the cooperative system is in state ξ_j can be written as [6, Eq. 5.23]

$$\begin{aligned} &\Pr(e|\xi_j,\underline{\beta}) \\ &= \frac{4F}{\pi\sqrt{M}}\int_0^{\frac{\pi}{2}} \exp\left(-\frac{b_M}{\sin^2\theta}\left(\beta_{SD}\bar{\gamma}_{SD}+\sum_{r\in\Psi_j}\beta_{RD}^{(r)}\bar{\gamma}_{RD}^{(r)}\right)\right)d\theta \\ &\quad + \frac{4F^2}{\pi}\int_{\frac{\pi}{4}}^{\frac{\pi}{2}} \exp\left(-\frac{b_M}{\sin^2\theta}\left(\beta_{SD}\bar{\gamma}_{SD}+\sum_{r\in\Psi_j}\beta_{RD}^{(r)}\bar{\gamma}_{RD}^{(r)}\right)\right)d\theta, \end{aligned} \quad (67)$$

where $b_M = \frac{3}{2(M-1)}$ and $F = 1-\frac{1}{\sqrt{M}}$. Following the same procedure as shown in Appendix B and averaging over the CSI $\underline{\beta}$, the average probability of symbol error in the state ξ_j can be derived at high SNRs as

$$\mathbb{E}_{\underline{\beta}}\{\Pr(e|\xi_j,\underline{\beta})\} \doteq \frac{a_{SD}\Gamma(t_{SD}+1)}{(b_M\bar{\gamma}_{SD})^{t_{SD}+1}} \prod_{r\in\Psi_j} \left\{ \frac{a_{RD}^{(r)}\Gamma\left(t_{RD}^{(r)}+1\right)}{\left(b_M\bar{\gamma}_{RD}^{(r)}\right)^{t_{RD}^{(r)}+1}} \right\} \times C_{t_{SD}+1+\sum_{r\in\Psi_j} t_{RD}^{(r)}+|\Psi_j|}, \quad (68)$$

where the constant C_n is defined in Eq. (69). Following similar lines as shown in Equations (60)-(63), the expression for

$$\begin{aligned}\mathbb{E}_{\underline{\beta}}\{\Pr(e|\xi_j,\underline{\beta})\} =& \frac{1}{\pi}\int_0^{\frac{(M-1)\pi}{M}} \mathbb{E}_{\underline{\beta}}\left\{\exp\left(-\frac{b_M}{\sin^2\theta}\left(\beta_{SD}\bar{\gamma}_{SD}+\sum_{r\in\Psi_j}\beta_{RD}^{(r)}\bar{\gamma}_{RD}^{(r)}\right)\right)d\theta\right\}\\ =& \frac{1}{\pi}\int_0^{\frac{(M-1)\pi}{M}}\int_0^{\infty}\exp\left(-\frac{b_M\beta_{SD}\bar{\gamma}_{SD}}{\sin^2\theta}\right)f_{\beta_{SD}}(\beta_{SD})d\beta_{SD}\prod_{r\in\Psi_j}\int_0^{\infty}\exp\left(-\frac{b_M\beta_{RD}^{(r)}\bar{\gamma}_{RD}^{(r)}}{\sin^2\theta}\right)f_{\beta_{RD}^{(r)}}\left(\beta_{RD}^{(r)}\right)d\beta_{RD}^{(r)}\\ =& \frac{1}{\pi}\int_0^{\frac{(M-1)\pi}{M}}\int_0^{\infty}\exp\left(-\frac{b_M\beta_{SD}\bar{\gamma}_{SD}}{\sin^2\theta}\right)\left[a_{SD}(\beta_{SD})^{t_{SD}}+o\left((\beta_{SD})^{t_{SD}+\epsilon}\right)\right]d\beta_{SD}\\ &\times\prod_{r\in\Psi_j}\int_0^{\infty}\exp\left(-\frac{b_M\beta_{RD}^{(r)}\bar{\gamma}_{RD}^{(r)}}{\sin^2\theta}\right)\left[a_{RD}^{(r)}\left(\beta_{RD}^{(r)}\right)^{t_{RD}^{(r)}}+o\left(\left(\beta_{RD}^{(r)}\right)^{t_{RD}^{(r)}+\epsilon}\right)\right]d\beta_{RD}^{(r)}. \qquad (64)\end{aligned}$$

$$\begin{aligned}C_n =& \frac{4F}{\pi\sqrt{M}}\int_0^{\frac{\pi}{2}}\sin^{2n}\theta d\theta+\frac{4F^2}{\pi}\int_{\frac{\pi}{4}}^{\frac{\pi}{2}}\sin^{2n}\theta d\theta\\ =& \frac{1}{n\pi}\left(1-\frac{1}{\sqrt{M}}\right)^2\left(\frac{1}{2}\right)^{n-1}\left\{1+\sum_{k=1}^{n-1}\frac{(2n-1)(2n-3)\cdots(2n-2k+1)}{(n-1)(n-2)\cdots(n-k)}\right\}\\ &+\frac{(2n-1)(2n-3)\cdots 1(M-1)}{2^n n!M}. \qquad (69)\end{aligned}$$

$\mathbb{E}_{\underline{\beta}}\{\Pr(\xi_j|\underline{\beta})\}$ considering M-QAM can be derived as

$$\begin{aligned}&\mathbb{E}_{\underline{\beta}}\{\Pr(\xi_j|\underline{\beta})\}\\ &\doteq\prod_{r\in\bar{\Psi}_j}\mathbb{E}_{\underline{\beta}}\{\Pr(\xi_j(r)|\underline{\beta})\}\\ &=\prod_{r\in\bar{\Psi}_j}\left[\frac{4F}{\pi\sqrt{M}}\int_0^{\frac{\pi}{2}}\mathbb{E}_{\underline{\beta}}\left\{\exp\left(-\frac{b_M}{\sin^2\theta}\left(\beta_{SR}^{(r)}\bar{\gamma}_{SR}^{(r)}\right)\right)d\theta\right\}\right.\\ &\quad\left.+\frac{4F^2}{\pi}\int_{\frac{\pi}{4}}^{\frac{\pi}{2}}\mathbb{E}_{\underline{\beta}}\left\{\exp\left(-\frac{b_M}{\sin^2\theta}\left(\beta_{SR}^{(r)}\bar{\gamma}_{SR}^{(r)}\right)\right)d\theta\right\}\right]\\ &=\prod_{r\in\bar{\Psi}_j}\left\{\frac{a_{SR}^{(r)}\Gamma(t_{SR}^{(r)}+1)}{(b_M\bar{\gamma}_{SR}^{(r)})^{t_{SR}^{(r)}+1}}\times C_{t_{SR}^{(r)}+1}\right\}. \qquad (70)\end{aligned}$$

Appendix D
Proof of Theorem 3

Similar to the $\mathcal{P}_0$ protocol, one can once again take recourse to the fundamental relationship for the average end-to-end SER, averaged over the instantaneous CSI $\underline{\beta}$ given as

$$\Pr(e)=\mathbb{E}_{\underline{\beta}}\{\Pr(e|\underline{\beta})\}=\sum_{j=0}^{2^R-1}\mathbb{E}_{\underline{\beta}}\{\Pr(e|\xi_j,\underline{\beta})\mathbb{E}_{\underline{\beta}}\{\Pr(\xi_j|\underline{\beta})\}, \qquad (71)$$

where the instantaneous CSI β for the $\mathcal{P}_m$ protocol is defined as $\underline{\beta}=\{\beta_{SD},\beta_{SR}^{(r)},\beta_{RD}^{(r)},\beta_{RR}^{(\tilde{r},\overline{r})},1\le r\le R,\max\{1,r-m\}\le\tilde{r}\le r-1\}$. The average probability of the system being in state ξ_j can be expressed as [16]

$$\mathbb{E}_{\underline{\beta}}\{\Pr(\xi_j|\underline{\beta})\}=\prod_{r=1}^{R}\Pr\big(\xi_j(r)\big), \qquad (72)$$

where the quantity $\Pr(\xi_j(r))$ is the average conditional probability of the relay r being in state $\xi_j(r)$ and can be defined for the $\mathcal{P}_m$ system as

$$\begin{aligned}\Pr(\xi_j(r))&=\mathbb{E}_{\underline{\beta}}\{\Pr(\xi_j(r)|\xi_j(r-1),\cdots,\xi_j(r-m),\underline{\beta}\}\\ &=\begin{cases}\mathbb{E}_{\underline{\beta}}\{P_{S\to R^{(r)}}(e^{(r)}|\underline{\beta})\} & \text{if } \xi_j(r)=0,\\ 1-\mathbb{E}_{\underline{\beta}}\{P_{S\to R^{(r)}}(e^{(r)}|\underline{\beta})\} & \text{if } \xi_j(r)=1.\end{cases} \qquad (73)\end{aligned}$$

The average probability of error $\mathbb{E}_{\underline{\beta}}\{P_{S\to R^{(r)}}(e^{(r)}|\underline{\beta})\}$ at relay r, can be evaluated as shown in (74). Exploiting now the fact that $1-(\cdot)\approx 1$ at high SNRs in (73), the expression for $\mathbb{E}_{\underline{\beta}}\{\Pr(\xi_j|\underline{\beta})\}$ in (72) can be simplified to

$$\begin{aligned}&\mathbb{E}_{\underline{\beta}}\{\Pr(\xi_j|\underline{\beta})\}\doteq\prod_{r\in\bar{\Psi}_j}\Pr(\xi_j(r))\\ &=\prod_{r\in\bar{\Psi}_j}\left\{\frac{a_{SR}^{(r)}\Gamma(t_{SR}^{(r)}+1)}{\left(b_M\bar{\gamma}_{SR}^{(r)}\right)^{t_{SR}^{(r)}+1}}\prod_{q\in\Psi_j(r)}\left\{\frac{a_{RR}^{(q,r)}\Gamma(t_{RR}^{(q,r)}+1)}{\left(b_M\bar{\gamma}_{RR}^{(q,r)}\right)^{t_{RR}^{(q,r)}+1}}\right\}\right.\\ &\quad\left.\times C_{t_{SR}^{(r)}+1+\sum_{q\in\Psi_j(r)}\left(t_{RR}^{(q,r)}+1\right)}\right\}. \qquad (75)\end{aligned}$$

Furthermore, it can be noted that the average probability of symbol error in the state ξ_j is identical to the one derived in (59) for the $\mathcal{P}_0$ protocol at high SNRs and is given as

$$\begin{aligned}\mathbb{E}_{\underline{\beta}}\{\Pr(e|\xi_j,\underline{\beta})\}\doteq&\frac{a_{SD}\Gamma(t_{SD}+1)}{(b_M\bar{\gamma}_{SD})^{t_{SD}+1}}\prod_{r\in\Psi_j}\left\{\frac{a_{RD}^{(r)}\Gamma\left(t_{RD}^{(r)}+1\right)}{\left(b_M\bar{\gamma}_{RD}^{(r)}\right)^{t_{RD}^{(r)}+1}}\right\}\\ &\times C_{t_{SD}+1+\sum_{r\in\Psi_j}t_{RD}^{(r)}+|\Psi_j|}. \qquad (76)\end{aligned}$$

Substituting both these results for $\mathbb{E}_{\underline{\beta}}\{\Pr(\xi_j|\underline{\beta})\}$ and $\mathbb{E}_{\underline{\beta}}\{\Pr(e|\xi_j,\underline{\beta})\}$ in the expression for the end-to-end SER in (71) derives the claim in the above theorem.

$$\begin{aligned}\mathbb{E}_{\underline{\beta}}\{P_{S\to R^{(r)}}(e^{(r)}|\underline{\beta})\} =&\frac{1}{\pi}\int_0^{\frac{(M-1)\pi}{M}} \mathbb{E}_{\underline{\beta}}\left\{\exp\left(-\frac{b_M}{\sin^2\theta}\left(\beta_{SR}^{(r)}\bar{\gamma}_{SR}^{(r)}+\sum_{q=\max(1,r-m)}^{r-1}\beta_{RR}^{(q,r)}\bar{\gamma}_{RR}^{(q,r)}\xi_j(q)\right)\right)d\theta\right\}\\ =&\frac{1}{\pi}\int_0^{\frac{(M-1)\pi}{M}}\left[\int_0^{\infty}\exp\left(-\frac{b_M\beta_{SR}^{(r)}\bar{\gamma}_{SR}^{(r)}}{\sin^2\theta}\right)f_{\beta_{SR}^{(r)}}\left(\beta_{SR}^{(r)}\right)d\beta_{SR}^{(r)}\right.\\ &\left.\times\prod_{q\in\Psi_j(r)}\exp\left(-\frac{b_M\beta_{RR}^{(q,r)}\bar{\gamma}_{RR}^{(q,r)}}{\sin^2\theta}\right)f_{\beta_{RR}^{(q,r)}}\left(\beta_{RR}^{(q,r)}\right)d\beta_{RR}^{(q,r)}\right]d\theta\\ \doteq&\frac{a_{SR}^{(r)}\Gamma(t_{SR}^{(r)}+1)}{\left(b_M\bar{\gamma}_{SR}^{(r)}\right)^{t_{SR}^{(r)}+1}}\prod_{q\in\Psi_j(r)}\left\{\frac{a_{RR}^{(q,r)}\Gamma(t_{RR}^{(q,r)}+1)}{\left(b_M\bar{\gamma}_{RR}^{(q,r)}\right)^{t_{RR}^{(q,r)}+1}}\right\}C_{t_{SR}^{(r)}+1+\sum_{q\in\Psi_j(r)}\left(t_{RR}^{(q,r)}+1\right)}. \end{aligned} \tag{74}$$

REFERENCES

[1] N. Varshney and A. K. Jagannatham, "A unified framework for the analysis of path selection based DF cooperation in wireless systems," in *Proc. IEEE WCNC*, 2017, pp. 1–6.

[2] J. N. Laneman, D. N. Tse, and G. W. Wornell, "Cooperative diversity in wireless networks: Efficient protocols and outage behavior," *IEEE Trans. Inf. Theory*, vol. 50, no. 12, pp. 3062–3080, 2004.

[3] A. Nosratinia, T. E. Hunter, and A. Hedayat, "Cooperative communication in wireless networks," *IEEE Commun. Mag*, vol. 42, no. 10, pp. 74–80, 2004.

[4] J. N. Laneman and G. W. Wornell, "Energy-efficient antenna sharing and relaying for wireless networks," in *Proc. IEEE WCNC*, vol. 1, 2000, pp. 7–12.

[5] G. Kramer, M. Gastpar, and P. Gupta, "Cooperative strategies and capacity theorems for relay networks," *IEEE Trans. Inf. Theory*, vol. 51, no. 9, pp. 3037–3063, 2005.

[6] K. R. Liu, *Cooperative communications and networking*. Cambridge University Press, 2009.

[7] Y. Zhao, R. Adve, and T. J. Lim, "Outage probability at arbitrary SNR with cooperative diversity," *IEEE Commun. Lett.*, vol. 9, no. 8, pp. 700–702, 2005.

[8] J. Hu and N. C. Beaulieu, "Closed-form expressions for the outage and error probabilities of decode-and-forward relaying in dissimilar Rayleigh fading channels," in *Proc. IEEE ICC*, 2007, pp. 5553–5557.

[9] Y. Li and S. Kishore, "Asymptotic analysis of amplify-and-forward relaying in Nakagami-fading environments," *IEEE Trans. Wireless Commun*, vol. 6, no. 12, pp. 4256–4262, 2007.

[10] E. Soleimani-Nasab, A. Kalantari, and M. Ardebilipour, "Performance analysis of multi-antenna DF relay networks over Nakagami-m fading channels," *IEEE Commun. Lett.*, vol. 15, no. 12, pp. 1372–1374, 2011.

[11] ——, "Performance analysis of selective DF relay networks over Rician fading channels," in *Proc. IEEE Symposium on Comput. and Commun. (ISCC)*. IEEE, 2011, pp. 117–122.

[12] Y.-W. P. Hong, W.-J. Huang, and C.-C. J. Kuo, *Cooperative communications and networking: technologies and system design*. Springer Science & Business Media, 2010.

[13] M. Hesam, A. Olfat, and N. C. Beaulieu, "Cooperative beamforming for two-hop multi-relay decode-and-forward networks," *IEEE Trans. Commun.*, vol. 63, no. 9, pp. 3143–3156, 2015.

[14] A. K. Sadek, W. Su, and K. R. Liu, "Multinode cooperative communications in wireless networks," *IEEE Trans. Signal Process*, vol. 55, no. 1, pp. 341–355, 2007.

[15] A. Hadjtaieb, A. Chelli, M.-S. Alouini, and H. Boujemaa, "Performance analysis of selective decode-and-forward multinode incremental relaying with maximal ratio combining," in *Proc. 2014 International Conference on Commun. and Netw. (ComNet)*. IEEE, 2014, pp. 1–6.

[16] N. Varshney, A. V. Krishna, and A. K. Jagannatham, "Selective DF protocol for MIMO STBC based single/multiple relay cooperative communication: End-to-end performance and optimal power allocation," *IEEE Trans. Commun.*, vol. 63, no. 7, pp. 2458–2474, 2015.

[17] H. Boujemaa, "Exact and asymptotic BEP of cooperative DS-CDMA systems using decode and forward Relaying in the presence of multipath propagation," *IEEE Trans. Wireless Commun*, vol. 8, no. 9, pp. 4464–4469, 2009.

[18] M. Fikadu, P. Sofotasios, S. Muhaidat, Q. Cui, G. Karagiannidis, and M. Valkama, "Error rate and power allocation analysis of regenerative networks over generalized fading channels," *IEEE Trans. Commun.*, 2016(Accepted for publication).

[19] Z. Wang and G. B. Giannakis, "A simple and general parameterization quantifying performance in fading channels," *IEEE Trans. Commun.*, vol. 51, no. 8, pp. 1389–1398, 2003.

[20] M. D. Yacoub, "The κ-μ distribution and the η-μ distribution," *IEEE Antennas Propag. Mag*, vol. 49, no. 1, pp. 68–81, 2007.

[21] A. K. Sadek, W. Su, and K. R. Liu, "A class of cooperative communication protocols for multi-node wireless networks," in *2005 IEEE 6th Workshop on Signal Processing Advances in Wireless Communications*. IEEE, 2005, pp. 560–564.

[22] A. Jeffrey and D. Zwillinger, *Table of integrals, series, and products*. Access Online via Elsevier, 2007.

[23] S. P. Boyd and L. Vandenberghe, *Convex optimization*. Cambridge University Press, 2004.

[24] M. Grant, S. Boyd, and Y. Ye, "CVX: MATLAB software for disciplined convex programming," 2008.

[25] N. Varshney, A. K Jagannatham, and L. Hanzo, "Technical Report: Asymptotic SER analysis and optimal power sharing for dual-phase and multi-phase multi-relay cooperative systems," Indian Institute of Technology Kanpur, Tech. Rep., 2018, [Online] http://www.iitk.ac.in/mwn/documents/MWNLab_TR_AError_2018.pdf

[26] A. Abdaoui, S. S. Ikki, and M. Ahmad, "Performance analysis of MIMO cooperative relaying system based on Alamouti STBC and amplify-and-forward schemes," in *Proc. IEEE ICC*, 2010, pp. 1–6.

[27] B. K. Chalise and L. Vandendorpe, "Outage probability analysis of a MIMO relay channel with orthogonal space-time block codes," *IEEE Commun. Lett.*, vol. 12, no. 4, pp. 280–282, 2008.

[28] A. Maaref and S. Aissa, "Shannon capacity of STBC in Rayleigh fading channels," *Electronics Lett.*, vol. 40, no. 13, pp. 817–819, 2004.

[29] M. H. Hassan and M. J. Hossain, "Cooperative beamforming for cognitive radio systems with asynchronous interference to primary user," *IEEE Trans. Wireless Commun.*, vol. 12, no. 11, pp. 5468–5479, 2013.

[30] J. Liu, W. Chen, Z. Cao, and Y. J. A. Zhang, "Cooperative beamforming for cognitive radio networks: A cross-layer design," *IEEE Trans. Commun.*, vol. 60, no. 5, pp. 1420–1431, 2012.

[31] T. M. Hoang, T. Q. Duong, H. A. Suraweera, C. Tellambura, and H. V. Poor, "Cooperative beamforming and user selection for improving the security of relay-aided systems," *IEEE Trans. Commun.*, vol. 63, no. 12, pp. 5039–5051, 2015.

[32] G. T. Djordjevic, M. I. Petkovic, A. M. Cvetkovic, and G. K. Karagiannidis, "Mixed RF/FSO relaying with outdated channel state information," *IEEE J. Sel. Areas Commun.*, vol. 33, no. 9, pp. 1935–1948, 2015.

[33] S. Anees and M. R. Bhatnagar, "On the capacity of decode-and-forward dual-hop free space optical communication systems," in *Proc. IEEE WCNC*, 2014, pp. 18–23.

[34] ——, "Performance of an amplify-and-forward dual-hop asymmetric RF–FSO communication system," *J. of Opt. Commun. and Netw.*, vol. 7, no. 2, pp. 124–135, 2015.

[35] K. P. Peppas and C. K. Datsikas, "Average symbol error probability of general-order rectangular quadrature amplitude modulation of optical wireless communication systems over atmospheric turbulence channels," *J. of Opt. Commun. and Netw.*, vol. 2, no. 2, pp. 102–110, 2010.

[36] S. Sanayei and A. Nosratinia, "Capacity maximizing algorithms for joint transmit-receive antenna selection," in *Proc. IEEE Asilomar*, vol. 2, 2004, pp. 1773–1776.

[37] L. Zhou and Y. Ohashi, "Recursive joint transmit and receive antenna selection in spatial multiplexing systems," in *Proc. IEEE VTC*, 2013, pp. 1–5.

[38] F. W. Olver, *NIST handbook of mathematical functions*. Cambridge University Press, 2010.

[39] A. Abdi, W. C. Lau, M.-S. Alouini, and M. Kaveh, "A new simple model for land mobile satellite channels: first-and second-order statistics," *IEEE Trans. Wireless Commun*, vol. 2, no. 3, pp. 519–528, 2003.

Neeraj Varshney (Student Member'10) received his B.Tech. degree in electronics and communication engineering from the Uttar Pradesh Technical University, Lucknow, India in 2008 and M.Tech. degree in electronics and communication engineering from the Jaypee Institute of Information Technology, Noida, India in 2011. He has submitted his Ph.D. thesis in electrical engineering department at the Indian Institute of Technology, Kanpur, India. Since May 2018 he is a visiting research fellow with the department of electrical engineering and computer science at Syracuse University, New York, USA. His research interests are in signal processing, communications and networks which include digital communication, MIMO technology, molecular communication in nano-networks. From Oct '11 to Aug '12, he was a project research fellow at Jaypee Institute of Information Technology Noida, India.

Aditya K. Jagannatham (Member'05) received his Bachelors degree from the Indian Institute of Technology, Bombay and M.S. and Ph.D. degrees from the University of California, San Diego, U.S.A.. From April '07 to May '09 he was employed as a senior wireless systems engineer at Qualcomm Inc., San Diego, California, where he worked on developing 3G UMTS/WCDMA/HSDPA mobile chipsets as part of the Qualcomm CDMA technologies division. His research interests are in the area of next-generation wireless communications and networking, sensor and ad-hoc networks, digital video processing for wireless systems, wireless 3G/4G cellular standards and CDMA/OFDM/MIMO wireless technologies. He has contributed to the 802.11n high throughput wireless LAN standard. He was awarded the CAL(IT)2 fellowship for pursuing graduate studies at the University of California San Diego and in 2009 he received the Upendra Patel Achievement Award for his efforts towards developing HSDPA/HSUPA/HSPA+ WCDMA technologies at Qualcomm. Since 2009 he has been a faculty member in the Electrical Engineering department at IIT Kanpur, where he is currently an Associate Professor, and is also associated with the BSNL-IITK Telecom Center of Excellence (BITCOE). At IIT Kanpur he has been awarded the P.K. Kelkar Young Faculty Research Fellowship (June 2012 to May 2015) for excellence in research and the Gopal Das Bhandari Memorial Distinguished Teacher Award for the year 2012-13 for excellence in teaching. He has also delivered a set of video lectures on Advanced 3G and 4G Wireless Mobile Communications for the Ministry of Human Resource Development funded initiative NPTEL (National Programme on Technology Enhanced Learning).

Lajos Hanzo (http://www-mobile.ecs.soton.ac.uk) FREng, FIEEE, FIET, Fellow of EURASIP, DSc received his degree in electronics in 1976 and his doctorate in 1983. In 2009 he was awarded an honorary doctorate by the Technical University of Budapest and in 2015 by the University of Edinburgh. In 2016 he was admitted to the Hungarian Academy of Science. During his 40-year career in telecommunications he has held various research and academic posts in Hungary, Germany and the UK. Since 1986 he has been with the School of Electronics and Computer Science, University of Southampton, UK, where he holds the chair in telecommunications. He has successfully supervised 111 PhD students, co-authored 18 John Wiley/IEEE Press books on mobile radio communications totalling in excess of 10 000 pages, published 1777 research contributions at IEEE Xplore, acted both as TPC and General Chair of IEEE conferences, presented keynote lectures and has been awarded a number of distinctions. Currently he is directing a 60-strong academic research team, working on a range of research projects in the field of wireless multimedia communications sponsored by industry, the Engineering and Physical Sciences Research Council (EPSRC) UK, the European Research Council's Advanced Fellow Grant and the Royal Society's Wolfson Research Merit Award. He is an enthusiastic supporter of industrial and academic liaison and he offers a range of industrial courses. He is also a Governor of the IEEE ComSoc and VTS. During 2008 - 2012 he was the Editor-in-Chief of the IEEE Press and a Chaired Professor also at Tsinghua University, Beijing. For further information on research in progress and associated publications please refer to http://www-mobile.ecs.soton.ac.uk